ABSTRACT

LEUNG, CHUN-KIT. Design Considerations of High Voltage and High Frequency 3 Phase Transformer for Solid State Transformer Application. (Under the direction of Dr. Subhashish Bhattacharya.)

The 3 phase Solid State Transformer (SST) is one of the key elements in the Future Renewable Electric Energy Delivery and Management (FREEDM) System where the center is headquartered on NC State University's Centennial Campus. One of the main purposes of the Solid State Transformer is to step up or down the voltages in the power system at higher frequency than the conventional 60 Hz frequency transformer, to achieve a reduction in size while maintaining high efficiency and high reliability merits. To transform the voltages at high frequency, the Solid State Transformer needs to consist of a rectifier, dual active bridge converters, a high frequency transformer and an inverter. There are two purposed topologies for the 3 phase transformer and each topology is designs at 3 kHz and 20 kHz, therefore the design of electromagnetic, thermal and mechanical analysis of the 3 phase transformer are conducted in this thesis. The proposed design of the transformer applications are validated with the simulation of Finite Element Analysis software. A conclusion ends with a comparison of advantages and disadvantages between the transformer designs to find the best application for the 3 phase Solid State Transformer project.

Design Considerations of High Voltage and High Frequency 3 Phase Transformer for Solid State Transformer Application

by
Chun-kit Leung

A thesis submitted to the Graduate Faculty of
North Carolina State University
in partial fulfillment of the
requirements for the Degree of
Master of Science

Electrical Engineering

Raleigh, North Carolina

2010

APPROVED BY:

_____	_____
Dr. Mesut Baran	Dr. Srdjan Lukic
Committee Member	Committee Member

_____
Dr. Subhashish Bhattacharya
Committee Chair

BIOGRAPHY

Chun-kit Leung is a master student, class of 2010, at North Carolina State University, major in Electrical Engineering with a concentration in Power System. He also graduated from North Carolina State University with a Bachelor of Science degree in Electrical Engineering in 2006. Right after he obtained his bachelor degree, he worked for Waukesha Electric System (WES), a power transformer manufacturer company in the US. He was employed as a transformer electrical design engineer for 3 years where he learned most of his liquid-immerse 3 phase power transformer designs. While employed at WES, he decided to further his education on a part-time basis in master degree in Electrical Engineering.

ACKNOWLEDGEMENTS

I would like to first give my appreciation to my committee chair professor Dr. Subhashish Bhattacharya. He led me into the design of high frequency transformer for Solid State Transformer. His extensive knowledge in power electronic and transformer area has guided and helped me throughout this paper. His enthusiasm in these areas has influences and motivated me into further and deeper finding in high frequency transformer.

I would like to thank Dr. Mesut Baran and Dr. Srdjan Lukic for being in my committee. Their generous assistances and advices have helped me along the way in completing this paper. Their expertise in different areas has given me a different view from other aspects.

I can not thank Tiefu Zhao and Seunghun Baek enough for providing a great deal of support in the considerations of Solid State Transformer and high frequency transformer. Their knowledge and experiences has helped me layout the foundation knowledge in SST and high frequency transformer. I hope my work will provides some help to them in their future building of 3 phase high frequency transformer.

It has been a great opportunity to contribute my work to the FREEDM project and has been a pleasure to work with all of the people mentioned above. Finally, I would like to thank my family, my friends and the one who loved me, to support and understand me unconditionally when I came across obstacles and became frustrated. These encouragements guided me to continue and overcome the challenges until the finish of this paper. Again, I

would like give my appreciations to the people mentioned above and also others who helped me in this paper.

TABLE OF CONTENTS

LIST OF TABLES

LIST OF FIGURES

CHAPTER 1

1. INTRODUCTION

Transformers are electrical devices which change or transform voltage levels between two circuits. In the modern power system grids, transformers step up or down the voltage at the frequency of 60 Hz between the transmission and distribution systems. However, these traditional transformers often require a large space for storage because one of the determining factors for sizing the transformer is operating frequency. By increasing the operating frequency, the transformer's core size can be reduced significantly therefore achieving smaller transformer size, lighter in weight and less material costs. There are numbers of limiting factors that prevent the use of much higher frequency than 20 kHz; Core losses and winding losses can be higher due to irregular stray flux and skin effect. These energy losses in the transformer appear as heat among the core and coils, and these heat must be dissipated without allowing the windings to reach a temperature which will cause excessive deterioration of the insulation. The continuous deterioration of the insulation can ultimately lead to dielectric breakdown in the transformer. The proposed transformer frequency is design for 3 kHz and 20 kHz at 33.3 kVA and 100 kVA ratings respectively.

The 3 phase transformer is connected between the dual active bridge (DAB) converters as part of the SST components. The Pulse Width Modulated square voltage waveforms are generated from the DAB and is injected into the input side terminals of the 3 phase transformer. These square voltage waveforms are undesirable in the traditional 3

phase 3 core limbs type design. These waveforms are consisting of infinite numbers of odd integer harmonics which produce undesired harmonic fluxes in the core yokes. As these additional harmonic fluxes migrate with the power frequency flux, the core will become saturated which lead to strayed flux escaping the core and induce into the metallic structures and dissipate into heat and causes localized heating. Contrarily, the conventional 3 phase sinusoidal voltages produce majority power frequency flux in the core which the flux of different phases overlap in the top or bottom yokes of the core, they cancel each other out. Thus the yoke steel does not have to be designed to carry more flux than is produced by a single phase and at any instant of time, the 3 voltage fluxes sum to zero. To avoid core saturation, the core design is implemented with the five-legged core form design which solves the problem of harmonic flux and stray flux from unbalanced voltages may leave the core and enter free space inside the transformer by providing magnetic flux paths around the three core legs between the top and bottom yokes. As example of the 5 legged-core shell-form design is shown below.

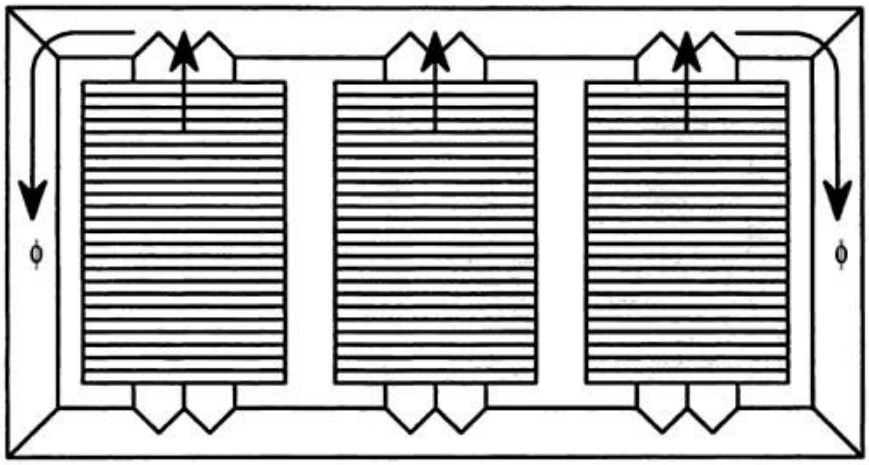

Figure 1 5 Legged Core Shell-Form Design

Residual flux, labeled Ø, consists of multiple of third harmonics, is the total flux arriving at the top core yoke from the core legs of the three phases. A fourth and fifth core leg provide two return paths for the residual flux from the top to the bottom yoke.

The insulation material needs to be robust enough to withstand the high voltage potential to ground at 11.4 kV. This challenge comes in as the core size decreases at high frequency, the available core window area also decreases, making the whole core and coils more compact. Different types of insulations are introduced to avoid any damaging electrical stresses exerted on the insulation materials.

CHAPTER 2

2. SOLID STATE TRANSFORMER TOPOLOGIES AND REQUIREMENTS FOR HIGH FREQEUNCY TRANSFORMER

2.1 3 phase Solid State Transformer Topology and operating principle

With the advancement of semiconductor technology, solid state transformer (SST) with high voltage fast switching SiC power devices is becoming a valid option to replace the conventional transformers in the power substation [1]. The main advantages to replace the conventional transformers with the solid state transformer are reduction in size and power quality improvement. The 3 phase solid state transformer consists of three stages AC/DC rectifier, a dual active bridge converter with a high frequency transformer and a DC/AC inverter, for each phase.

There are two proposed topologies for the SST. The outline of topology 1 is described as follow:

A 3 phase SST rated at 33.3kVA connected to a 12 kV distribution voltage with center-tapped 480V three phase output, the figure is shown below.

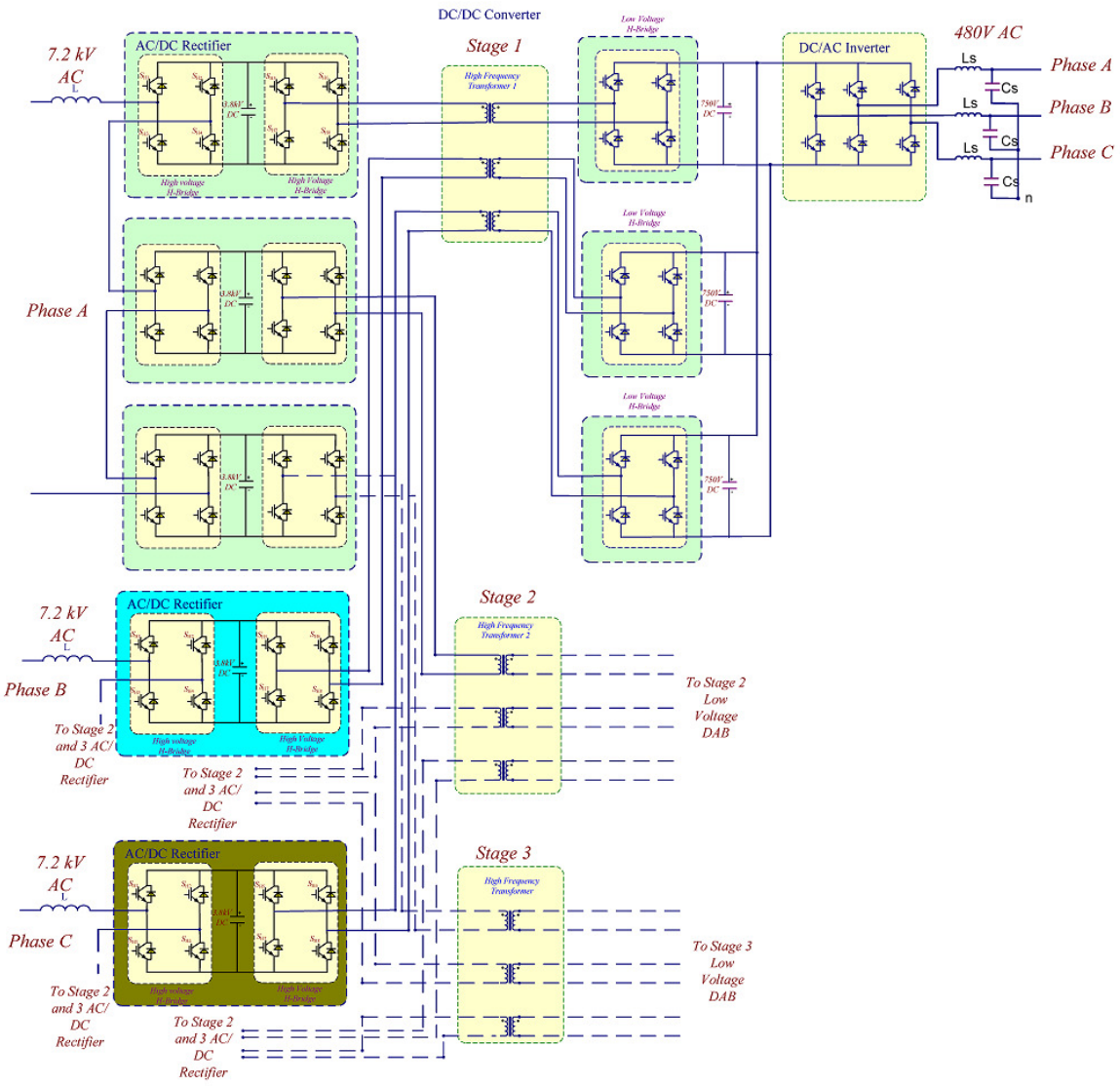

Figure 2 SST Topology 1 Diagram

The SST's input voltage is three phase at 7.2kV, 60 Hz, output voltage at 480 V, 60 Hz, 3 phase/3 wires. Each phase of the SST consists of a three cascaded high voltage high frequency AC/DC rectifier that converts 60 Hz, 7.2 kV AC to three 3.8 kV DC buses, three high voltage high frequency DC-DC converters that convert 3.8 kV to 750V with the help of the high frequency transformer, the 750V DC bus is converted to 480V AC 60 Hz, 480 V, 3

phase/3 wires by a voltage source inverter (VSI). The switching devices in high voltage H-bridge and low voltage H-bridges in Fig. 2 are 6.5 kV silicon IGBT and 600 V silicon IGBT respectively. The switching frequency of the high voltage silicon IGBT devices is 3 kHz, and the low voltage IGBT in the VSI switches at 10 kHz [2].

The topology 2 is envisioned as a step up future design in voltage class and power rating of the topology 1. The three cascaded 3.8 kV AC/DC rectifiers are combined into one 11.4 kV rectifier and the power rating steps up to 100 kVA combined in 3 phases SST. This topology requires the replacement of silicon based (Si) devices in the AC-AC converter with new devices which have higher voltage withstand ability at higher frequency switching and higher temperature operation capability devices, such as Silicon-Carbide based (SiC) devices. On the same token, the high frequency transformer steps up to 100 kVA, 11.4 kV - 750 V, is required. The core window area available becomes more stringent as the number of turns in the primary winding increased by three folds. The topology 2 diagram is shown below.

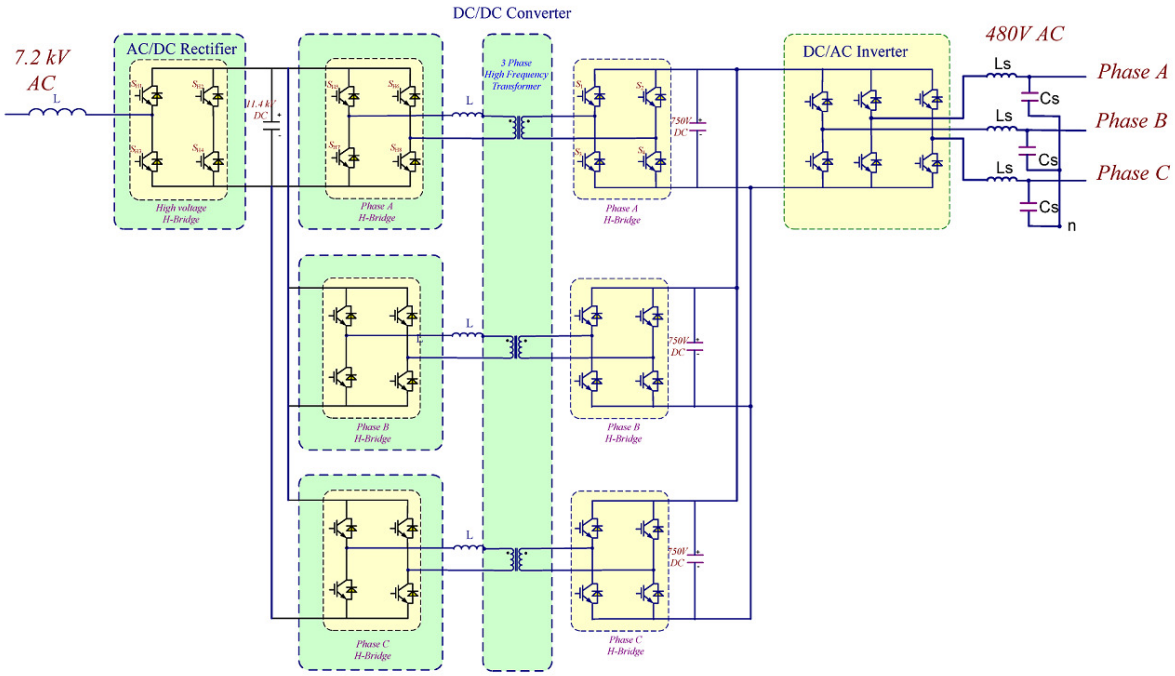

Figure 3 SST Topology 2 Diagram

The dual active bridge (DAB) converter topology offers zero voltage switching for all the switches, relatively low voltage stress for the switches, low passive component ratings and complete symmetry of configuration that allows seamless control for bidirectional power flow. Real power flows from the bridge with leading phase angle to the bridge with lagging phase angle, the amount of power transferred being controlled by the phase angle difference and the magnitudes of the dc voltages at the two ends as given by [3].

$$P_o = \frac{V_{dc} V_{dc\_link}}{2\pi f L} \phi \left(1 - \frac{|\phi|}{\pi}\right)$$

Where, V is input and output DC voltage, f is the frequency, L is the leakage inductance from the transformer, ϕ is the phase shift between input and output bridges.

2.2 Required Leakage Inductance with respect to Operating Frequency

The leakage inductance of the transformer is used as one of the components to transfer power within the DAB. The power transfer equation (2.1.1) is shown in the previous section. From the equation, the high leakage inductance required is relatively large and the geometry of the transformer needs to be very large in order to meet the leakage inductance requirements which will be discussed in the latter part of this thesis. An external inductor is needed to achieve the require inductance. The leakage inductance required for power transfer within the DAB for different ratings and topologies are given below in Table 1, 2, 3 & 4. The phase shifts are evaluated at $\pi/6$ for the most optimum performance.

Table 1 Rating Specification of Topology 1 at 3 kHz

	High Voltage Side	Low Voltage Side
DC-bus [V]	3800	750
Power [W]	11.11 kW	
Switching frequency [f]	3000	
Phase Shift [ϕ]	$\pi/6$	
Leakage Inductance [L]	0.030084	

Table 2 Rating Specification of Topology 1 at 20 kHz

	High Voltage Side	Low Voltage Side
DC-bus [V]	3800	750
Power [W]	11.11 kW	
Switching frequency [f]	20000	

Table 2 Continued

Phase Shift [ϕ]	$\pi/6$
Leakage Inductance [L]	0.004513

Table 3 Rating Specification of Topology 2 at 3 kHz

	High Voltage Side	Low Voltage Side
DC-bus [V]	11400	750
Power [W]	33.33 kW	
Switching frequency [f]	3000	
Phase Shift [ϕ]	$\pi/6$	
Leakage Inductance [L]	0.090251	

Table 4 Rating Specification of Topology 2 at 20 kHz

	High Voltage Side	Low Voltage Side
DC-bus [V]	11400	750
Power [W]	33.33 kW	
Switching frequency [f]	20000	
Phase Shift [ϕ]	$\pi/6$	
Leakage Inductance [L]	0.013538	

CHAPTER 3

3 CORE MATERIAL AND STRUCTURE SELECTION

3.1 Core Material Comparison

A magnetic core is a piece of magnetic material with a high permeability used to confine and guide magnetic fields in transformer. The high permeability, relative to the surrounding air, causes the magnetic field lines to be concentrated in the core material. The magnetic field is created by the primary coil of wire around the core that carries a current. The magnetic field of a coil can increase by a several thousand times when the core is presence.

The use of core material needs to be carefully chosen for high frequency application. The high frequency transformer causes flux to distribute unevenly throughout the core cross-sections, thus the flux crowding in non-uniform core cross sections and near sharp interior corners which lead to additional core losses and localized heating.

When the waveform of the flux is not sinusoidal, harmonic components of flux will cause an increase in core loss and exciting current because of increased eddy currents and skin effect. These increases become comparatively large if the exciting current is forced to approach sinusoidal shape at moderate and high inductions, because then the flux wave form will be approaching relatively square wave shape. Since harmonic components of flux cause increases in both the “in-phase” and quadrature components of exciting current, the operating a-c flux –current loop will be somewhat widened and altered in shape from that for sinusoidal flux. It is important to find a core material that has a low coercivity means the

material's magnetization can easily reverse direction without dissipating much energy (hysteresis losses), while the material's resistivity to remain high to prevents eddy currents in the core due to circulating currents induce by the varying flux.

The comparison between Silicon steel, Amorphous Alloy and Nanocrystalline material is discussed below. Ferrite material is left out of this discussion because of its low saturation flux density around typically 0.3-0.5 Tesla which does not allow high flexibility of designs.

3.1.1 Silicon Steel

Silicon Steel is an iron alloy which has around 0 to 6.5% silicon (Si:5Fe) property. Silicon significantly increases the electrical resistivity of the steel, which decreases the induced eddy currents and thus reduces the core loss. Silicon Steel is a popular core material for power transformer applications because of its high saturation flux density, high permeability and high manufacturing capability. The saturation flux density is close to 2 Tesla [4]. However, since the laminations of the silicon steel is usually around 7 – 11 mils, the eddy current and skin effect can cause the losses to be very high for 3 kHz and 20 kHz frequency range. Below is a figure to show the core losses increase tremendously at higher frequency range which generate excessive heating in the core.

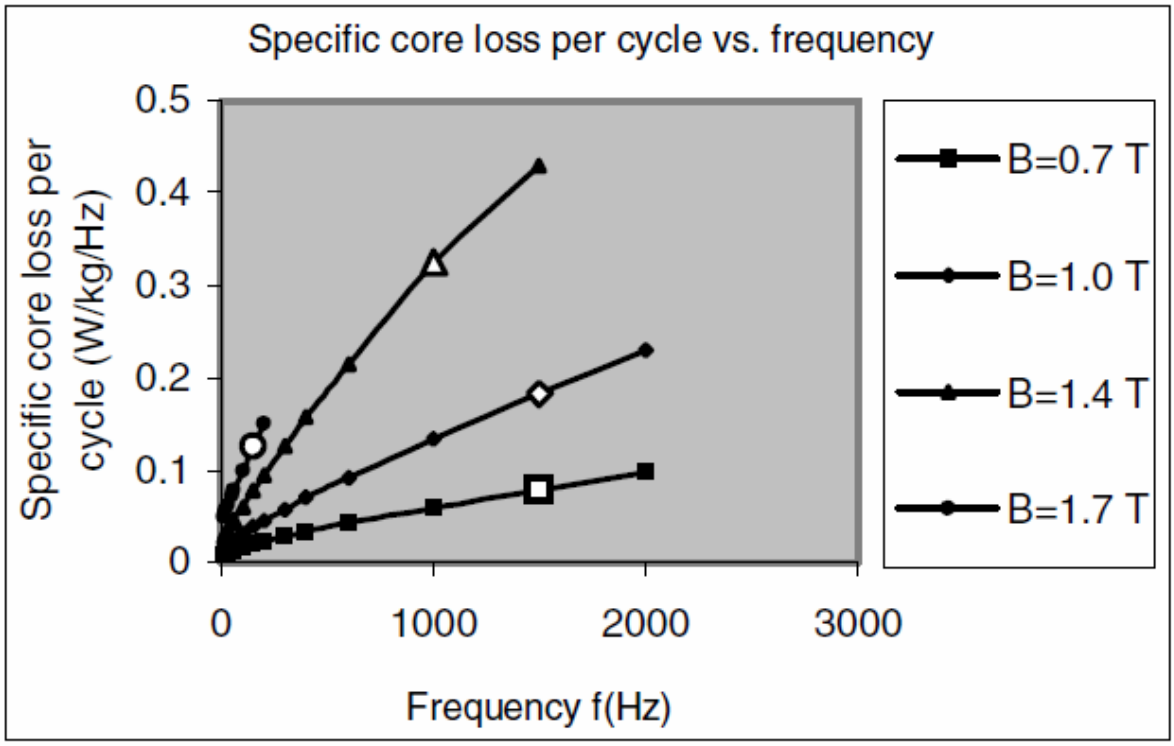

Figure 4 Core Loss per Watt/Kilogram/Hertz versus Frequency and Flux Density of Silicon Steel (Thickness 11 mils)

3.1.2 Amorphous Alloy

Amorphous alloy material is a metallic glass prepared by pouring molten alloy steel on a rotating cooled wheel, which cools the metal so quickly that crystals do not form. This material, also known as Metglas®, was commercialized in the early 1980s and used for low-loss power distribution transformer. The Metglas® is composed of 80% iron and 20% boron and a room temperature saturation magnetization of 1.56 Tesla [5]. The core loss can be 70%-80% less than silicon steel material. The Metglas®'s Powerlite® C-core has a wide range of high frequencies and hot-spot temperatures up to 155 degree Celsius. Its thermal limit is close to that of winding conductor's thermal limit (150 degree Celsius), so the

thermal design of the transformer can be best optimized. Its high saturation flux density range can add flexibility when designing the number of turns between the primary and secondary windings. The core cross-sectional area can also reduce to the minimum by increasing the flux density while within the thermal limits. Because of its high performance characteristics, this core material is chosen for the 3 kHz and 20 kHz transformer design.

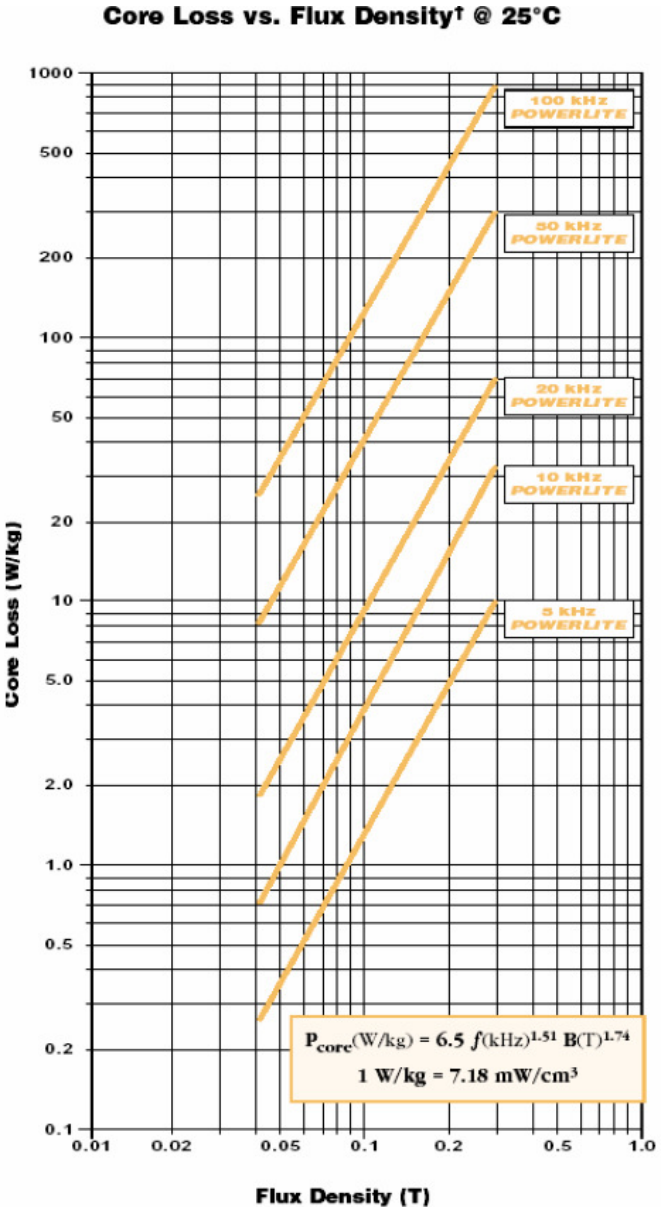

Figure 5 Core Loss (Watt/kilogram) versus Flux Density (Tesla) and Frequency for Metglas 2605SA1 Core

3.1.3 Nanocrystalline

Nanocrystalline soft magnetic material is prepared by crystallizing amorphous ribbons of specific families of iron and boron based alloy properties. This material offers

great soft magnetic properties: extremely low coercivities, high permeabilities (around 1.0 Tesla), low energy losses, etc. Application of these materials are in cores of transformers in switched-mode power supplies, chokes, ISDNs, etc., due to its high performance in the kilo Hertz frequency range [6]. Its permeability is higher by an approximate factor of 10 than that for a typical ferrite material, this means that there is a higher main inductance resulting in lower magnetization currents. As demonstration in figure 3 [6], the core loss is the lowest among the three materials at the 20 kHz range. However, due to its maximum operating temperature only range to 120 Celsius. This material is the limiting thermal factor compare to the winding conductor limit (150 C). Due to its high permeability, the core size is smaller than that of other materials, the heat dissipation is therefore concentrated across the small core surface causing the core temperature higher. Despite, the material cost is the highest of all three materials discussed above, it is necessary to use nanocrystalline material for more stringent designs. All of the toroidal uncutted tape-wound cores, oval and rectangle designs with or without cut are available to meet different design requirement needs.

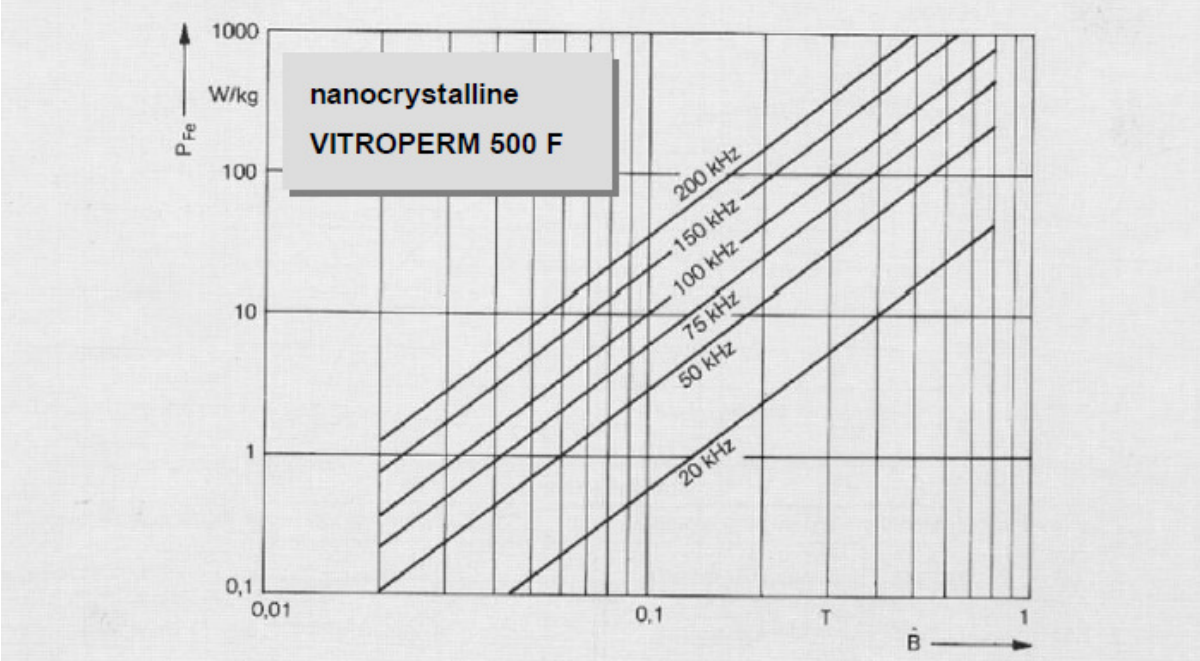

Figure 6 Core Loss per KG versus Flux Density of Vitroperm 500 F

3.2 Core Selection for Operating Frequency of 3 kHz and 20 kHz

After reviewing the material characteristics in the previous section, it makes sense to choose a core material which has a high performance while maintaining manufacturability and cost of material aspects. The Metglas® Powerlite® C-core design offers both of these requirements, its product catalog gives wide ranges of off-the-shelf core design for flexibility. The proposed five legged-core for the 3 phase transformer can be composed of eight Powerlite® C-cores with both primary and secondary windings wound on the same core leg. A fourth and fifth core leg provide two return paths for the residual flux from the top to the bottom yoke. The top and bottom core yokes is made with a reduced cross-sectional area because they do not have to carry the full complement of flux from each phase. This has the advantage of reducing the overall height of the transformer. The disadvantage of reducing

the cross-sectional area of the yokes is that a portion of the normal flux from the outer phases must now flow through the fourth and fifth core legs. This makes the actual flux path uncertain and makes calculating core losses difficult. The figures below shows the third harmonic effect on 3 core limb design as all of the third harmonic fluxes flow in the same direction and the 5 core limb design provides extra magnetic paths for the third harmonic fluxes to flow.

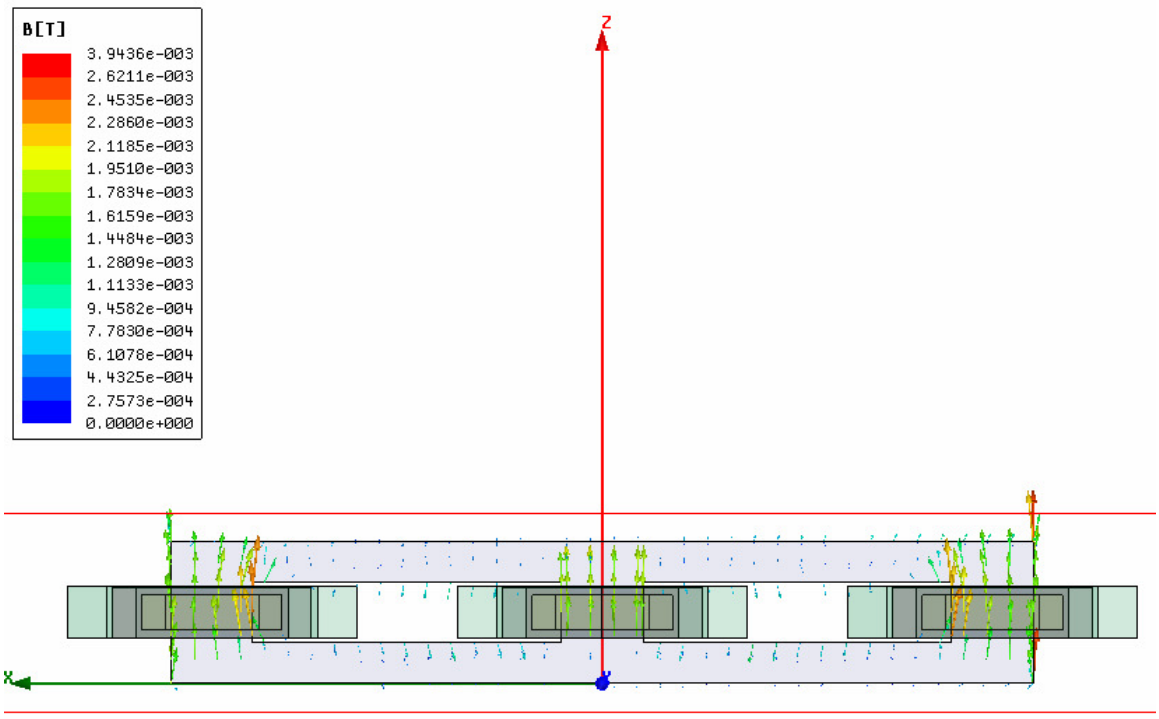

Figure 7 Third Harmonic Effect on 3 Core Limb design

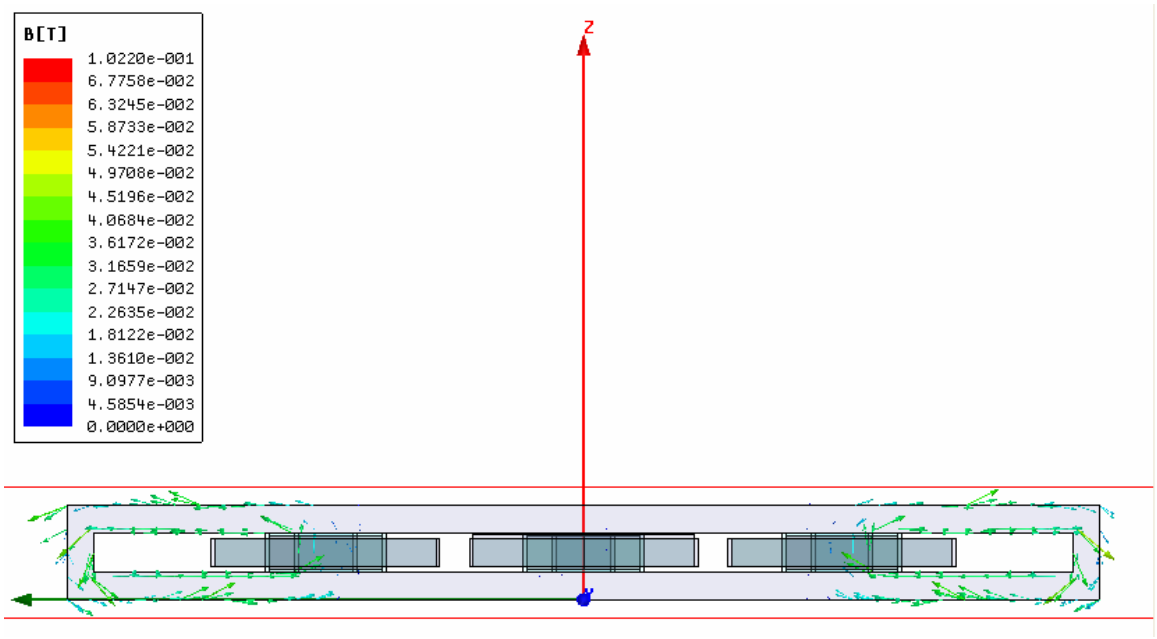

Figure 8 Third Harmonic Effect on 5 Core Limb design

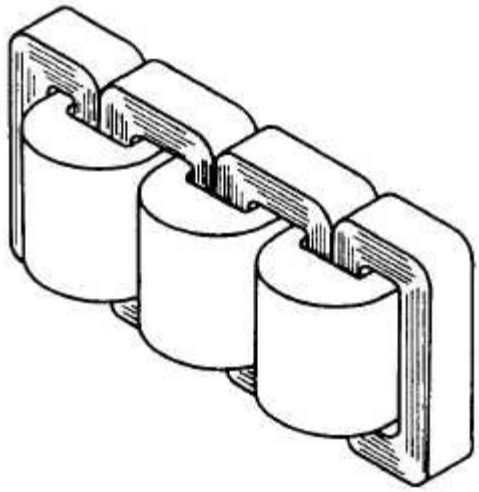

Figure 9 Proposed 5-Legged Shell-Form Design

Dimensions, Geometry and BH curve are shown below to showcase the Powerlite® AMCC C-core design which is used for this transformer design.

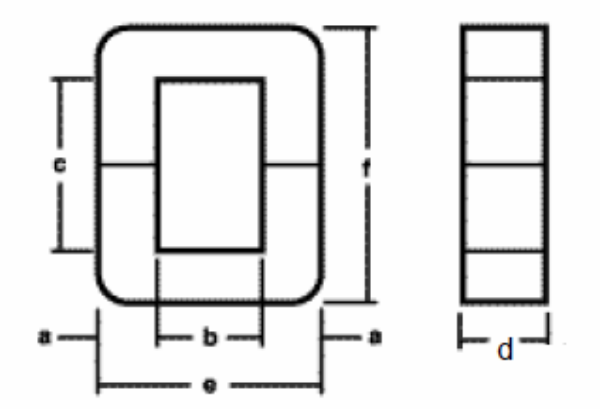

Figure 10 Geometry of Metglas AMCC C-Core

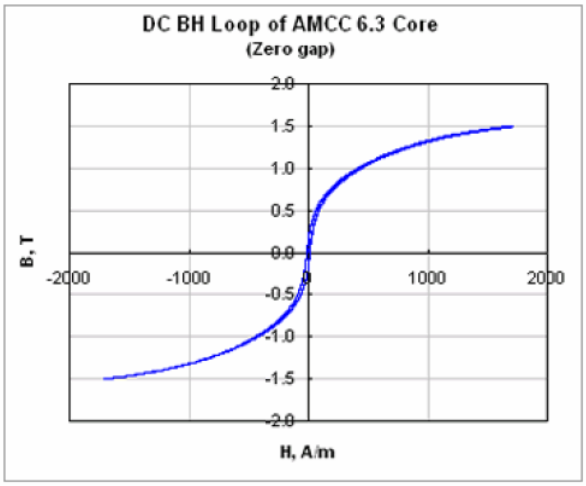

Figure 11 B-H curve of Metglas AMCC C-Core

Table 5 Dimensions of AMCC1000 and AMCC168S Powerlite® C-core

	Core Dimension [mm]						Performance Parameters			
	a	b	c	d	e	f	Length path [cm]	Core area [cm^2]	Window area [cm^2]	Mass [g]
AMCC1000	33.0	40.0	105.0	85.0	106.0	171.0	42.7	23.0	42.0	7109
AMCC168S	204	30	154.2	20	70.5	195.0	45.4	3.35	45.8	1109

The leakage inductance represents energy stored in the non-magnetic regions; majority between the primary and secondary windings, cause by imperfect flux coupling. Because of the limited window space in the core, the primary winding is wound on top of the secondary winding of each phase; therefore the leakage inductance is relatively small between the windings. Thus, an external inductor is required to meet the leakage inductance requirements for the power transfer within the dual active bridge converter for all designs. Inductor designs are discussed in the latter part of the thesis.

3.3 Wire Selection

The primary and secondary coils are wound around the core legs. The magnet wire should be self insulated from the aspects of turn to turn voltage stress to avoid any corona inception voltage during the life of the transformer. Polyurethane insulated is chosen for the insulation of the conductor with Polyamide (Nylon) overcoat to provide mechanical protection during winding and insertion. To avoid corona generated from the conductor, a design practice of no more than 200V between turn to turn is applied. A picture is shown for illustration of the magnet wire from Rea Magnet Wire Company. The round shape conductor is chosen because of the ease of skin depth calculation in circular radius which will discuss in this section.

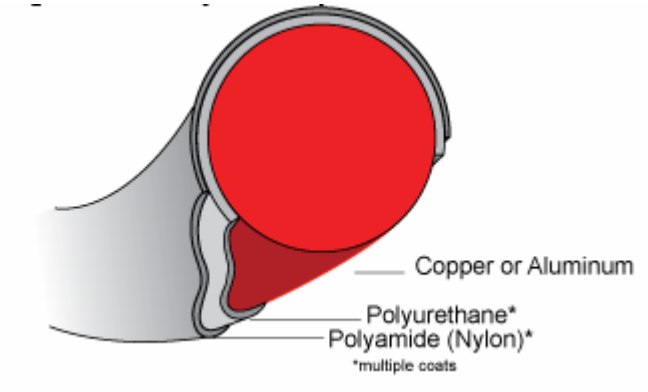

Figure 12 Conductor Insulated with Polyurethane and Nylon coatings

Table 6 Specification of Rea® Nysol® conductor

Magnet Wire Type	Rea® Wire Company Nysol® conductor
Shape of Conductor	Round
Electrical Insulation	Polyurethane
Thermal Class	155 C
Dielectric Breakdown	8.5 kV @ Room temperature 6.0 kV @ 155 C

In alternating electric current system under high frequency, skin effect has the tendency to concentrate its current to the surface of the conductor, at an average depth called the skin depth. Since the center part of the conductor has less effective area for the current to flow, meaning the same current will see more resistance within the conductor, the I^2R loss will be higher for high frequency current than that of direct current. Skin depth is defined as the distance below the surface where the current density has fallen to 1/e or 37% of its value at the surface. So it is important to size the conductor within the skin depth value, hence, all of the conductor area is fully utilized for the flow of current.

For copper at 70C:

$$S = \frac{2837}{\sqrt{f}}$$, where f is frequency in Hertz and S is the Skin depth in mils.

For the application of 3 kHz and 20 kHz, the skin depth is 51 mils and 20 mils respectively. Therefore conduct size needs to be a minimum of 9 AWG and 19 AWG (American Wire Gauge standard).

Table 7 Wire Size and DC Resistance of Topology 1 - 33.3 kVA 3 kHz design

	LV	HV
Wire Gauge [AWG]	17	15
Insulation	Polyurethane	
DC resistance [ohm/km] @ 20 C	16.61	10.45

Table 8 Wire Size and DC Resistance of Topology 1 - 33.3 kVA 20 kHz design

	LV	HV
Wire Gauge [AWG]	26	26
Insulation	Polyurethane	
DC resistance [ohm/km] @ 20 C	133.9	133.9

Table 9 Wire Size and DC Resistance of Topology 2 - 100 kVA 3 kHz design

	LV	HV
Wire Gauge [AWG]	26	26
Insulation	Polyurethane	
DC resistance [ohm/km] @ 20 C	133.9	133.9

Table 10 Wire Size and DC Resistance of Topology 2 - 100 kVA 20 kHz design

	LV	HV
Wire Gauge [AWG]	26	26
Insulation	Polyurethane	
DC resistance [ohm/km] @ 20 C	133.9	133.9

3.4 Winding Structure Selection

For shell-form transformers, there are two main methods of winding the coils. Both types are cylindrical coils, having an overall rectangular cross-section. In a disk coil, the turns are arranged in horizontal layers called disks which are wound alternately ou-in, in-out, etc. The winding is usually continuous so that the last inner or outer turn gradually transitions between the adjacent layers. When the disks are wound axially around the core, the winding is called a helical winding. The turns within a disk are usually touching so that a double layer of insulation separates the metallic conductors [8].

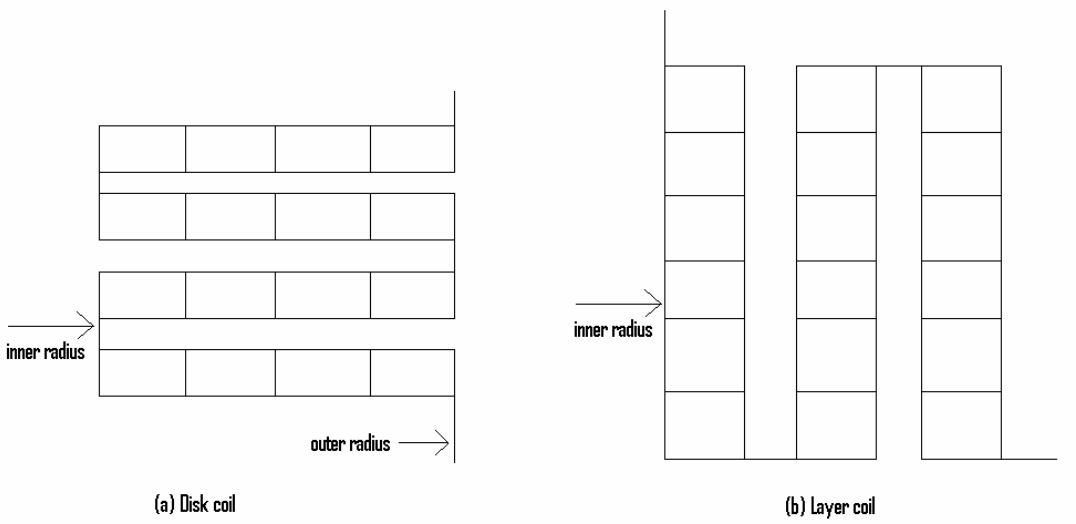

Figure 13 Disk and Layer Winding Configurations

The winding configurations of both primary and secondary windings are chosen to be layer wound, due to the round shape of the conductors. The round shape conductor does not have mechanical stability to stay next to the conductor radically. The round shape conductor was chosen because of the ease of skin depth calculation in circular radius.

Layers of insulation need to be placed between low voltage (LV) to core, low voltage winding layer to layer, low voltage winding (LV) to high voltage winding (HV), high winding layer to layer, high voltage winding to winding of different phases. Below is a cross-sectional view of winding configurations implemented for this design.

The picture is color-coded: The low voltage winding in this example is a two layers, four turns, five conductors connected in parallel in green color and a second turn of the same layer is wound right next to it, shown in magenta color. The high voltage winding configures as three layers, thirty-six turns and single strand conductor winding. This will be the winding nomenclature for the rest of the transformer designs for easy understanding.

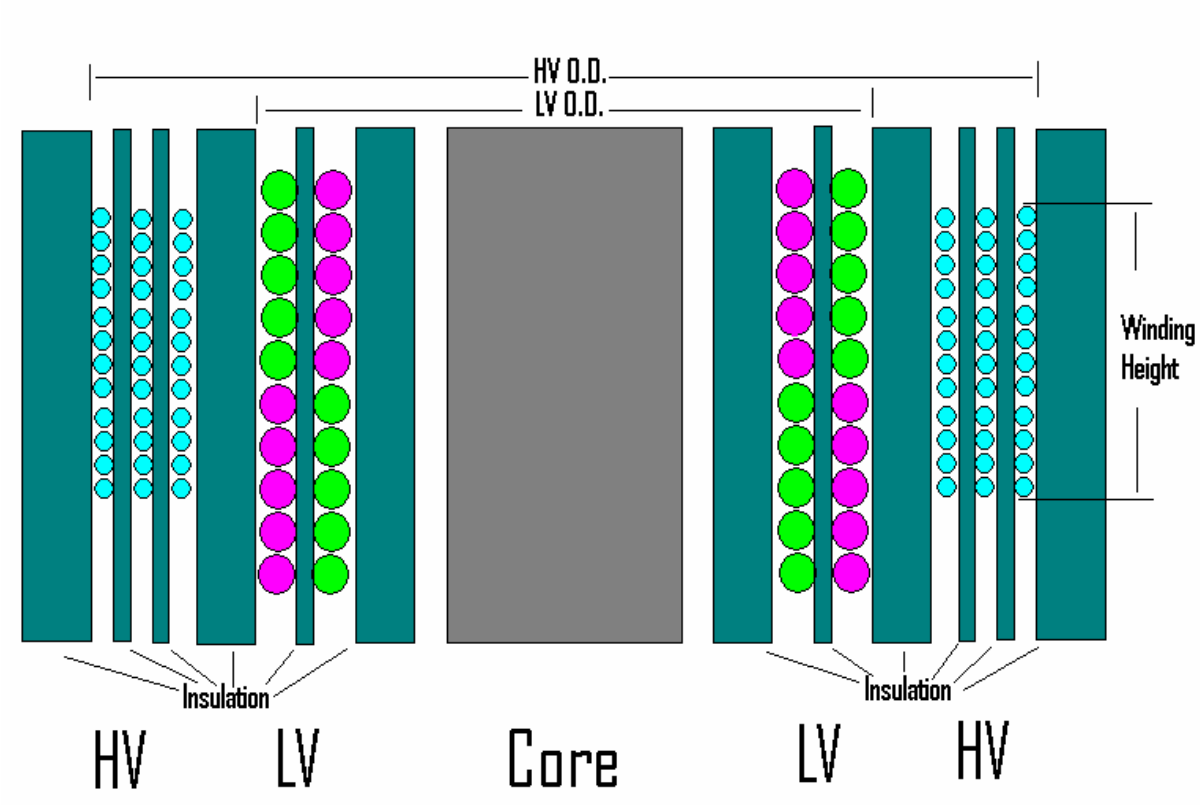

Figure 14 Layer Winding Configuration

Below show the specifications of the windings for Topology 1 & 2 and different ratings.

Table 11Winding Specifications of Topology 1- 33.3kVA 3 kHz

	LV	HV
Phase Voltage [V]	750	3800
Phase Current [A]	14.789	2.92
Wire Gauge [AWG]	17	15
# of Conductors in Parallel	5	1

Table 11 Continued

Copper Area [mm^2]	5.194	1.652
Turns	33	163
# of Turns per Layer	4	12
Winding Height [mm]	25.4	18.9
Conductor Length (all 3 Phases) [m]	158.53	234.64
Conductor Weight [kg]	7.32	3.44
Resistance (all 3 Phases) [Ω] @ 100 C	0.1384	3.223
Current Density [amp/cm^2]	285	177

Table 12 Winding Specifications of Topology 1 - 33.3 kVA 20 kHz

	LV	HV
Phase Voltage [V]	750	3800
Phase Current [A]	14.789	2.92
Wire Gauge [AWG]	26	26
# of Conductors in Parallel	26	9
Copper Area [mm^2]	3.346	1.158
Turns	50	251
# of Turns per Layer	2	5
Winding Height [mm]	25.1	21.7
Conductor Length (all 3 Phases) [m]	706.86	2216.80
Conductor Weight [kg]	21.01	22.82

Table 12 Continued

Resistance (all 3 Phases) [Ω] @ 100 C	0.184	4.817
Current Density [amp/cm^2]	442	252

Table 13 Winding Specifications of Topology 2 - 100 kVA 3 kHz

	LV	HV
Phase Voltage [V]	750	11400
Phase Current [A]	44.41	2.92
Wire Gauge [AWG]	16	17
# of Conductors in Parallel	13	1
Copper Area [mm^2]	16.995	1.039
Turns	20	293
# of Turns per Layer	2	16
Winding Height [mm]	36.3	25.5
Conductor Length (all 3 Phases) [m]	235.6	391.7
Conductor Weight [kg]	35.50	3.62
Resistance (all 3 Phases) [Ω] @ 100 C	0.024	8.552
Current Density [amp/cm^2]	261	282

Table 14 Winding Specifications of Topology 2 - 100 kVA 20 kHz

	LV	HV
Phase Voltage [V]	750	11400
Phase Current [A]	44.41	2.92
Wire Gauge [AWG]	26	26
# of Conductors in Parallel	100	10
Copper Area [mm^2]	12.870	1.287
Turns	24	355
# of Turns per Layer	1/2	5
Winding Height [mm]	24.13	24.13
Conductor Length (all 3 Phases) [m]	1627.53	4728.46
Winding Weight [kg]	186.1	54.1
Resistance (all 3 Phases) [Ω] @ 100 C	0.0286	8.322
Current Density [amp/cm^2]	345	227

CHAPTER 4

4 LOSS, TEMPERATURE AND ELECTROMAGNETIC ANAYLSIS OF LAYER WINDING TRANSFORMER DESIGN

4.1 Core Loss

Hysteresis and eddy-current losses are the main components of the core loss of a transformer. The hysteresis, as the name implies, means that the present state of a ferromagnetic material depends on its past magnetic history. The magnetic state of the core traverses the hysteresis loop, counterclockwise, once each cycle of the source frequency. Ferrous cores consist of billions of current dipoles, each with a north and south pole, that can rotate when the magnetic intensity cyclically reverses. The energy required to do this is converted to heat within the core and this energy is proportional to the area enclosed by the hysteresis loop [9]. Since the core is stacked with laminations, the flux in the core induces circulating current proportionally with the excitation frequency, so the eddy-currents loss increases as the square of the excitation frequency assumed the core material is pure resistive and conductive. And the resistive part of the core can be reduced by having very thin sheets of laminations because the eddy-current paths are now broken up resulting in a quite-small eddy-current power loss. The eddy-current loss then can be treated as I^2R losses are converted to heat. The sum of the hysteresis and eddy-current losses is the core loss. The core loss equation is given by Metglas® Powerlite® brochure and is listed below to calculate the core loss for different designs [10].

$$Pcore(\frac{W}{kg}) = 6.5 * f(kHz)^{1.51} * B(T)^{1.74}$$

$$1\frac{W}{kg} = 7.18\frac{mW}{cm^3}$$

Table 15 Core Loss of Topology 1 33.3 kHz 3 kHz

Switching Frequency [kHz]	3
Bac [T]	0.3
Type of Core	AMCC1000
Mass of a pair of AMCC1000 [kg]	7.109
Total Mass [kg]	28.436
Core Loss per Kilogram [W/kg]	4.203
Total core loss [W]	119.516

Table 16 Core Loss of Topology 1 33.3 kHz 20 kHz

Switching Frequency [kHz]	20
Bac [T]	0.2
Type of Core	AMCC168S
Mass of a pair of AMCC168S [kg]	1.101
Total Mass [kg]	4.404
Core Loss per Kilogram [W/kg]	36.413
Total core loss [W]	145.652

Table 17 Core Loss of Topology 2 100 kHz 3 kHz

Switching Frequency [kHz]	3
Bac [T]	0.5
Type of Core	AMCC1000
Mass of a pair of AMCC1000 [kg]	7.109
Total Mass [kg]	28.436
Core Loss per Kilogram [W/kg]	10.223
Total core loss [W]	290.699

Table 18 Core Loss of Topology 2 100 kHz 20 kHz

Switching Frequency [kHz]	20
Bac [T]	0.2
Type of Core	AMCC168S
Mass of a pair of AMCC168S [kg]	1.101
Total Mass [kg]	13.212
Core Loss per Kilogram [W/kg]	36.413
Total core loss [W]	481.093

4.2 Winding Loss

Although the transformer losses comprise a small percentage of the power in a transformer, yet these losses can produce localized heating which can compromise its operation. It is important to be able to calculate these losses at the design stage so that

adequate cooling can be provided. Winding loss is consists of resistive loss and stray losses. The resistive loss is I^2R loss in the windings and leads caused by the main current flow. Since the skin effect has been taken into account when choosing the conductor wire size, the winding loss can be easily calculated as direct current;

$$P_{dc} = I^2 R$$

The stray loss is the result of the stray flux from the windings and other metallic objects such as tank walls, etc. The stray loss depends on the conductivity, permeability, and shape of the metal object encountered. These losses are primarily due to induced eddy currents in these objects [8]. The stray loss on the conductor is given as follow:

$\%Eddy = 0.5(0.245 * f * t^2 * 2)^2$, where f = frequency, t = thickness of the conductor

$$\text{Stray loss} = \%\text{Eddy} * I^2R \text{ loss}$$

Finally the sum of resistive and stray loss of both primary and secondary windings gives the total winding loss.

$$P_{total} = (I^2R)_{pri} + (\text{Stray loss})_{pri} + (I^2R)_{sec} + (\text{Stray loss})_{sec}$$

Table 19 Winding Loss of Topology 1 - 33.3 kVA 3 kHz

	LV	HV
Phase Current	14.789	2.92
Wire Gauge [AWG]	17	15
Resistance (all 3 Phases) [Ω] @ 100 C	0.1384	3.223
Winding Loss (all 3 Phases) [w]	30.3	27.5

Table 19 Continued

% Eddy Loss	18.3	43.2
Winding loss [w]	35.85	39.38
Total Winding Loss [w]	75.23	

Table 20 Winding Loss of Topology 1 - 33.3 kVA 20 kHz

	LV	HV
Phase Current	14.789	2.92
Wire Gauge [AWG]	26	26
Resistance (all 3 Phases) [Ω] @ 100 C	0.184	4.817
Winding Loss (all 3 Phases) [w]	40.24	41.10
% Eddy Loss	16.9	16.9
Winding Loss [w]	47.04	48.05
Total Winding Loss [w]	95.09	

Table 21Winding Loss of Topology 2 - 100 kVA 3 kHz

	LV	HV
Phase Current	44.41	2.92
Wire Gauge [AWG]	16	17
Resistance (all 3 Phases) [Ω] @ 100 C	0.024	8.552
Winding Loss (all 3 Phases) [w]	47.49	73.12

Table 21 Continued

% Eddy Loss	26.8	18.3
Winding Loss [w]	60.22	86.5
Total Winding Loss [w]	146.72	

Table 22 Winding Loss of Topology 2 - 100 kVA 20 kHz

	LV	HV
Phase Current	44.41	2.92
Wire Gauge [AWG]	26	26
Resistance (all 3 Phases) [Ω] @ 100 C	0.0326	8.910
Winding Loss (all 3 Phases) [w]	64.35	76.18
% Eddy Loss	16.93	16.93
Winding Loss [w]	75.24	89.08
Total Winding Loss [w]	164.33	

4.3 Thermal Analysis

Energy losses in a transformer appear as heat in the core and coils. This heat must be dissipated without allowing the windings to reach a temperature which will cause excessive deterioration of the insulation.

To the user temperatures in a transformer are important for the determination of the amount of overload and the length of time that overload can be applied, how much "life" of the transformer has been or will be destroyed by operation at various temperatures. The

designer must be able to predict the temperature at all points in a transformer in order to determine that amount of copper to place in the coils, the type of cooling and insulation structures need to prevent excessive hot spots, the type and arrangement of internal and external cooling.

One of the challenges of high frequency design is the heat dissipation on effective cooling surfaces. As the core and coils decrease in size in high frequency applications, the amount of cooling surfaces decreases therefore, the core and coils will get hotter as a whole. The main cooling method for these transformer designs is natural convection that is the heat generated from core and coils get transfer to air through effective cooling surface area. Alternately, cooling fans maybe needed for higher losses designs.

The temperature limits for conductor and core are 155 C and 150 C respectively. The Nomex® and Kapton® insulations temperature limits are well above 200 C. The design temperatures for each component should be around 130 C and allow 20 C for localize hottest spot temperature with 30 C ambient temperatures. The hottest spot temperature is a localize heating area where non-uniform stray flux induces on the conductors usually near the end of the windings and the main flux concentrated on the inner concern of the core causes higher in flux density in the core. The temperature analysis is simulated by software, Ansoft® ePhysics®, using the winding and core losses calculated in the previous section. The actual dimension model is simulated with a conservative assumption: rectangular blocks modeled as windings since a rectangular block has less surface area than the surface area of a winding that consists of hundreds of individual conductors. In the model, each of the windings is enclosed by dielectric insulations to account for heat is thermally trapped by physical objects.

Below are the tables of temperatures calculated by ePhsyics® and the thermal analyses for each of the designs. Note that, the insulation objects are visually turned to transparent to show the temperatures of the windings underneath the insulations.

Table 23 Temperatures simulated by Ansoft® ePhyics®

	Topology 1 33.3 kVA 3 kHz	Topology 1 33.3 kVA 20 kHz	Topology 2 100 kVA 3 kHz	Topology 2 100 kVA 20 kHz	Max Allowable Temp [C]
Method of Cooling	Air	Air	Air	10" Dia. Fan @ 1075 RPM	N/A
Core [C]	80	110	90	115	150
High Voltage Winding [C]	68	107	98	104	155
Low Voltage Winding [C]	91	116	95	112	155

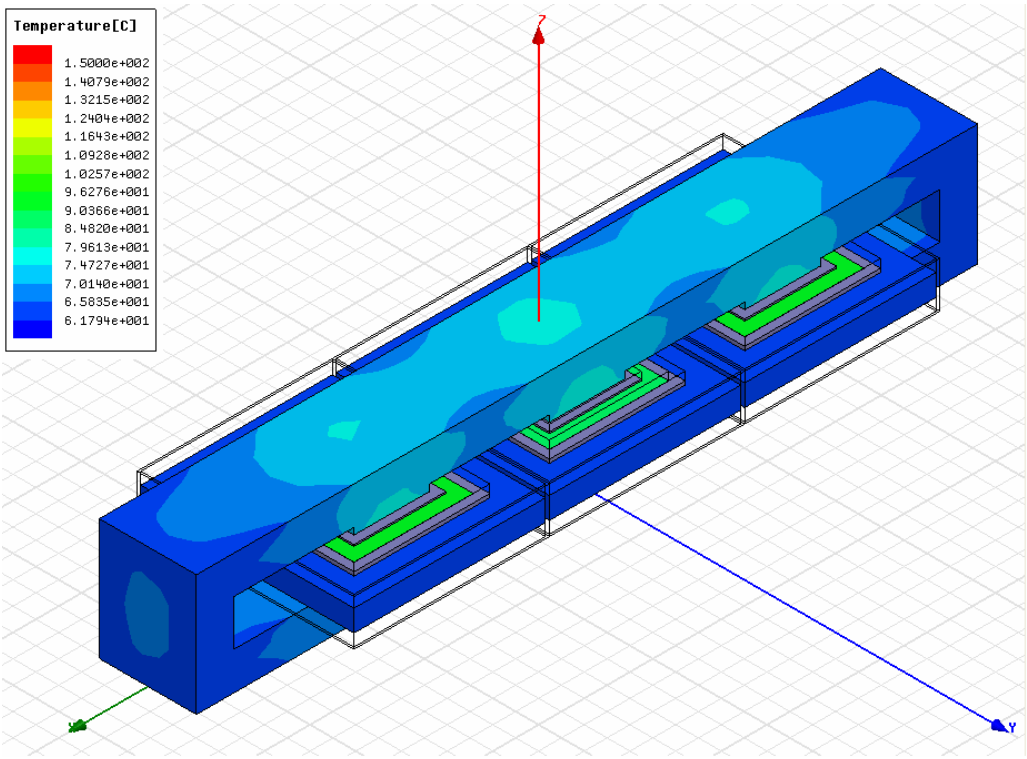

Figure 15 Temperature Simulation of Topology 1 - 33.3 kVA 3 kHz in 3D View

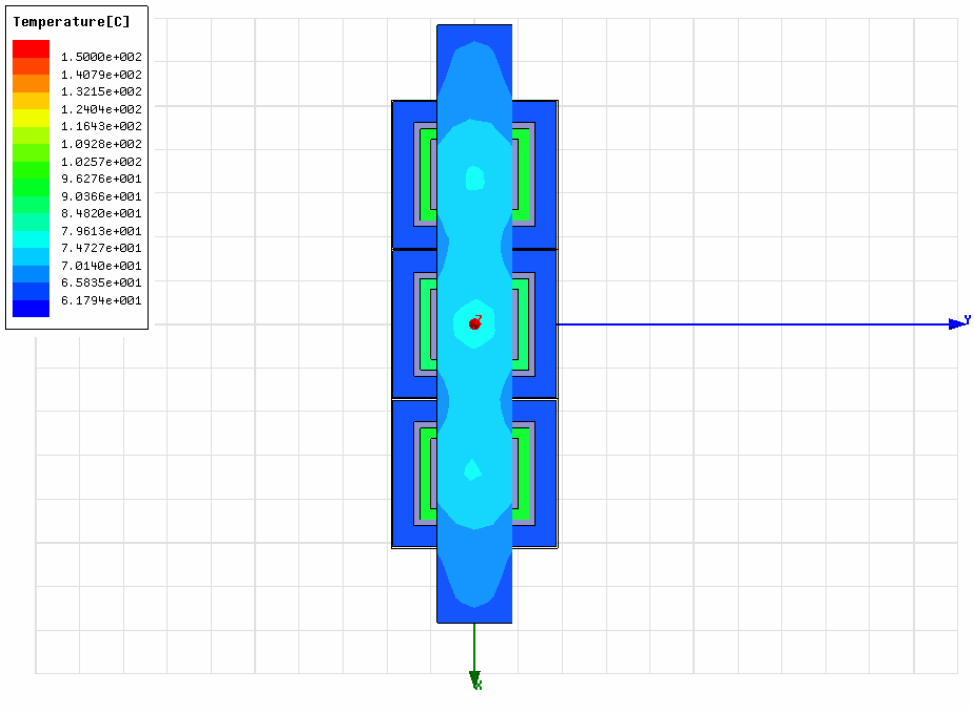

Figure 16 Temperature Simulation of Topology 1 - 33.3 kVA 3 kHz in Top View

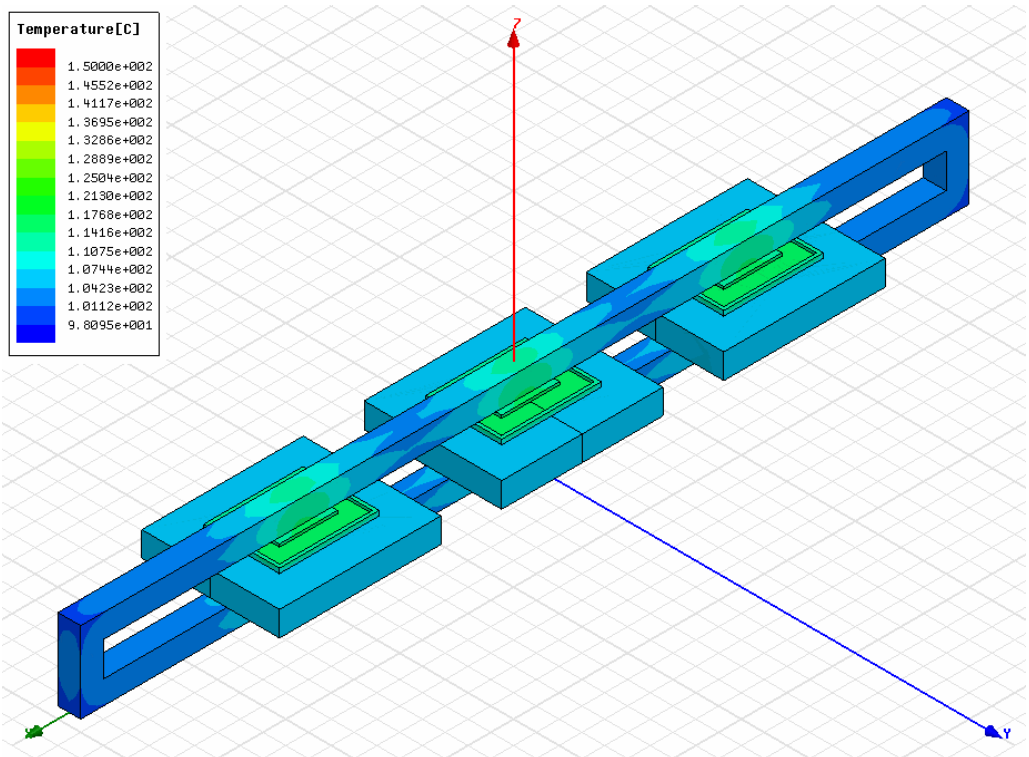

Figure 17 Temperature Simulation of Topology 1 - 33.3 kVA 20 kHz in 3D View

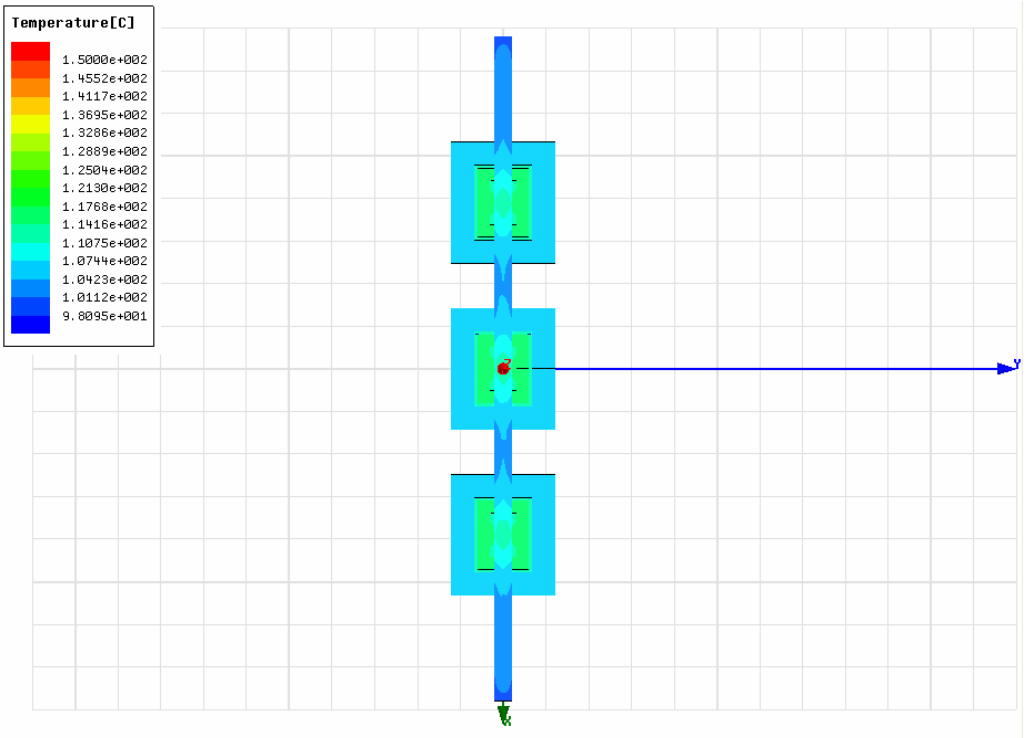

Figure 18 Temperature Simulation of Topology 1 - 33.3 kVA 20 kHz in Top View

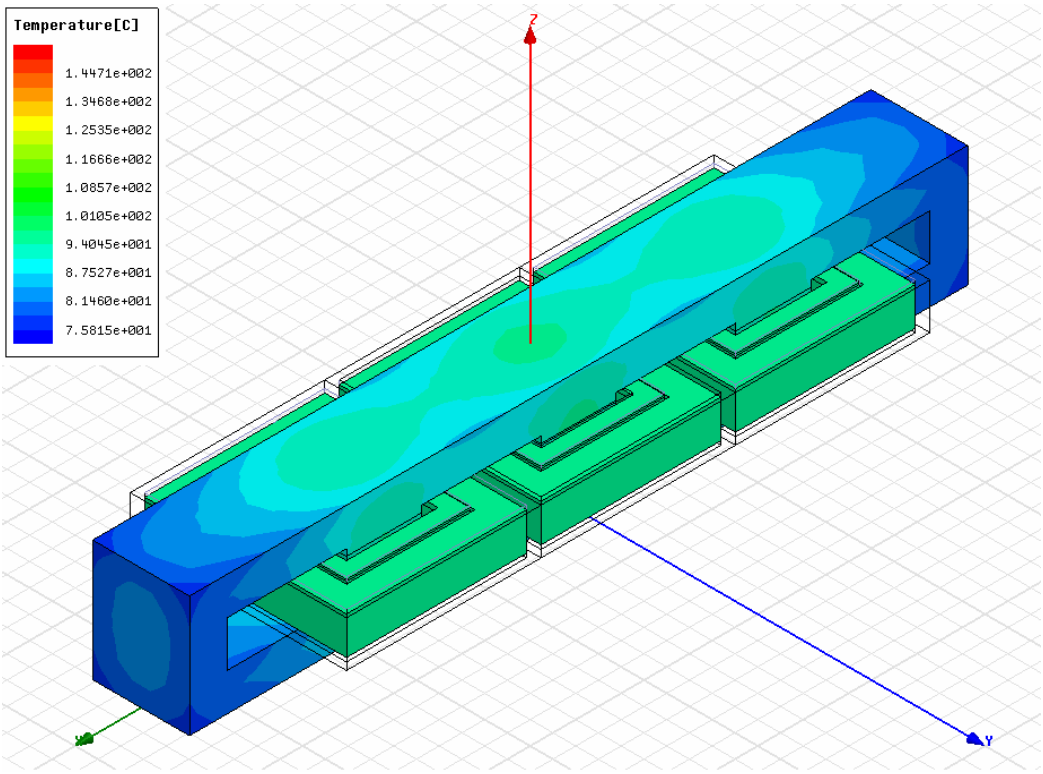

Figure 19 Temperature Simulation of Topology 2 - 100 kVA 3 kHz in 3D View

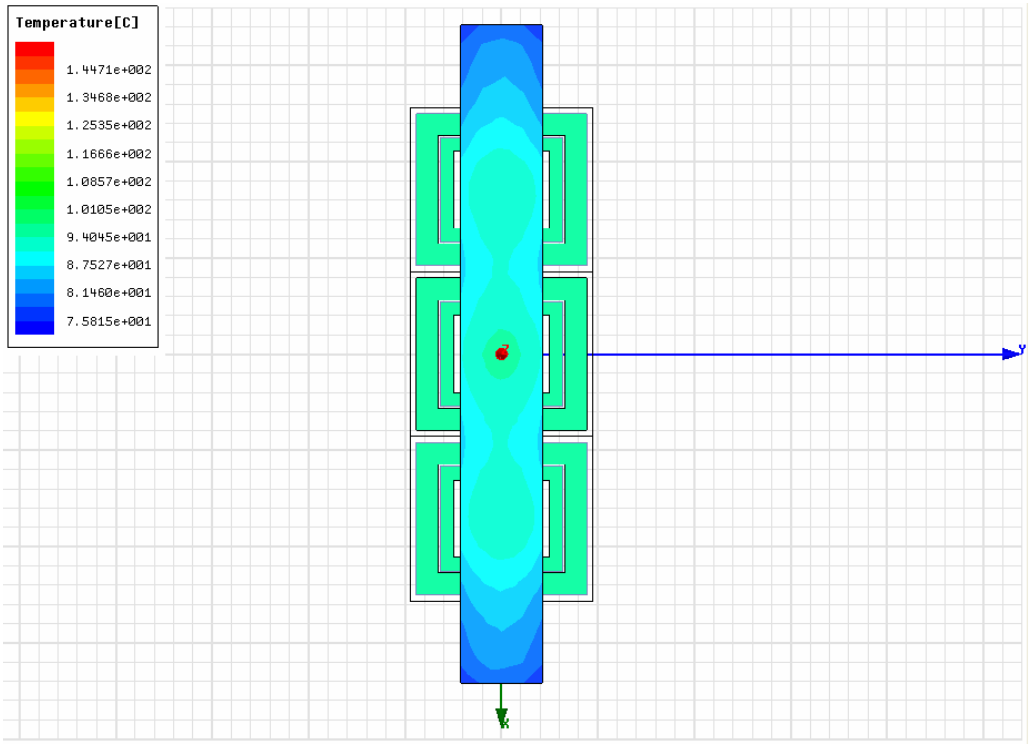

Figure 20 Temperature Simulation of Topology 2 – 100 kVA 3 kHz in Top View

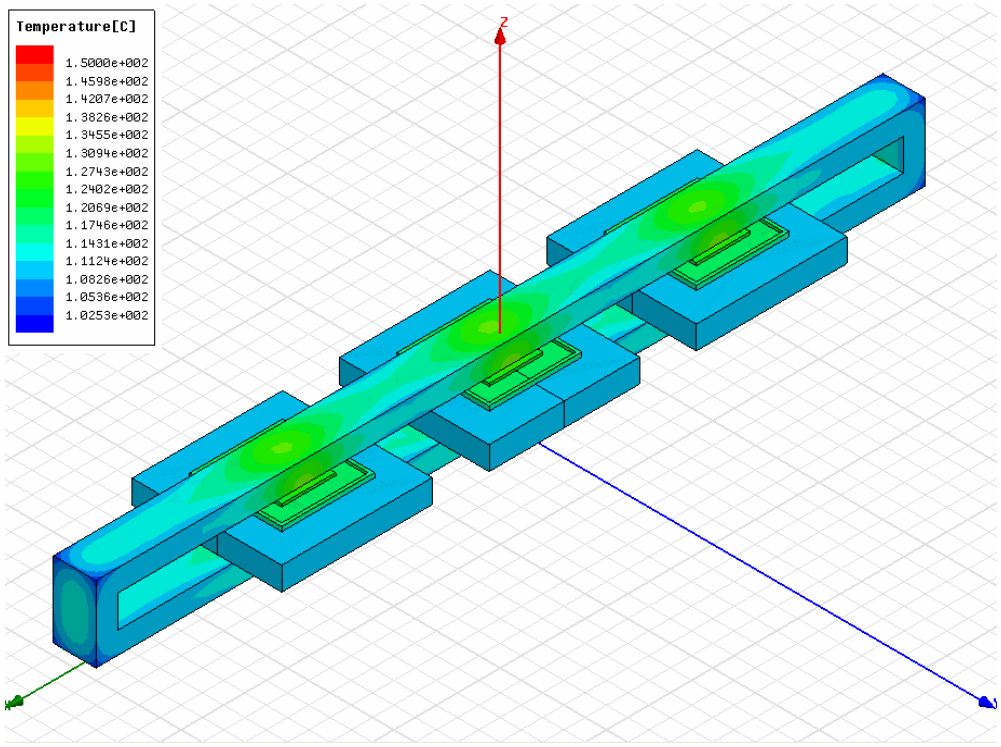
Temperature[C]
1.5000e+002
1.4598e+002
1.4207e+002
1.3826e+002
1.3455e+002
1.3094e+002
1.2743e+002
1.2402e+002
1.2069e+002
1.1746e+002
1.1431e+002
1.1124e+002
1.0826e+002
1.0536e+002
1.0253e+002
Z

Figure 21 Temperature Simulation of Topology 2 – 100 kVA 20 kHz in 3D View

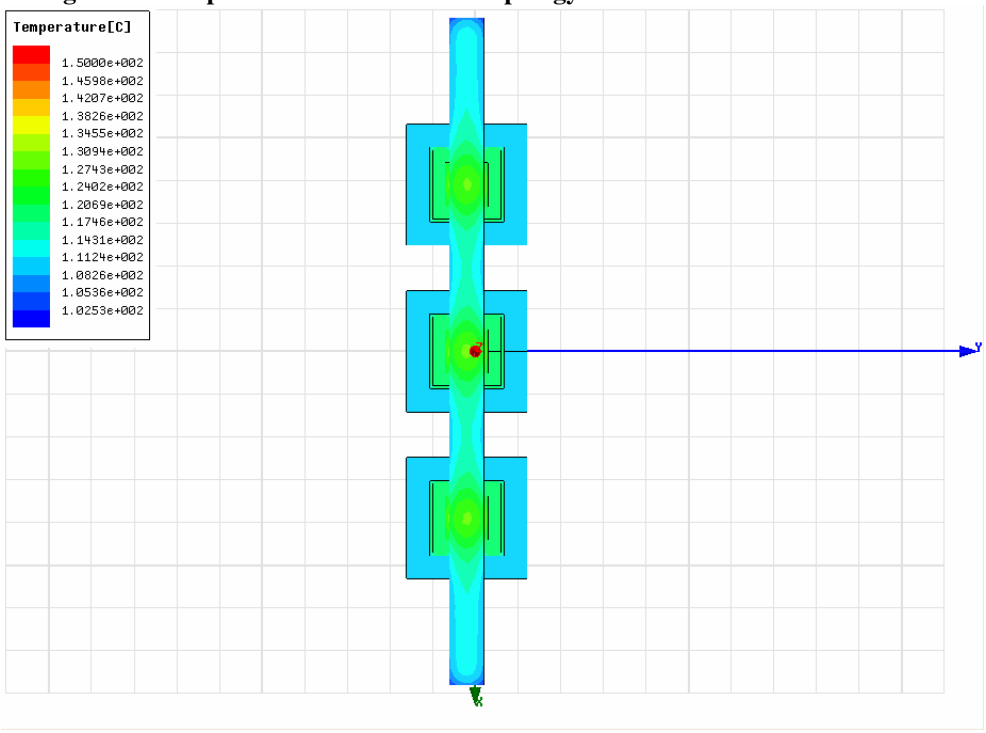

Figure 22 Temperature Simulation of Topology 2 – 100 kVA 20 kHz in Top View

4.4 Inductance Analysis

The dual active bridge consists of a high voltage H-Bridge, a high frequency transformer and a low voltage H-bridge. The rectifier controls the high voltage DC link voltage and the input current to be sinusoidal from the AC input. The low voltage DC link is regulated b the DAB converter.

The dual active bridge topology offers zero voltage switching for all the switches, relatively low voltage stress for the switches, low passive component ratings and complete symmetry of configuration that allows seamless control for bidirectional power flow. Real

power flows from the bridge with leading phase angle to the bridge with lagging phase angle, the amount of power transferred being controlled by the phase angle difference and the magnitudes of the dc voltages at the two ends as given by the following equation [3].

$$P_o = \frac{V_{dc} V_{dc\_link}}{2\pi fL} \phi (1 - \frac{|\phi|}{\pi})$$

Where, V is input and output DC voltage, f is the frequency, L is the leakage inductance from the transformer, ϕ is the phase shift between input and output bridges. So it is important to achieve an accurate leakage inductance when design the transformer.

4.4.1 Magnetic Field Distributions in Core

The magnetic field distribution in the five-legged three-phase core is analysis in this section. The main reason to reason a five-legged core is to provide a return path for third-harmonic flux. However, the problem introduced by this construction is that the actual flux paths are uncertain, and calculation of the core loss is likewise uncertain. The uncertainty of the flux paths is due to the fact that the top and bottom yokes are not large enough to carry the whole flux from one leg as the three-legged core. Although the natural tendency is for the flux to follow the three-legged pattern, the yokes saturate and force excess flux to "spill over" into the outer legs. This but will contain additional harmonic components. Exact calculation of the flux distribution and variation becomes practically impossible [11]. For this reason, it is a good practice to design the flux density in the core in the lower region to avoid saturation. The five-legged core design ensures all fluxes capture within the core at any given time.

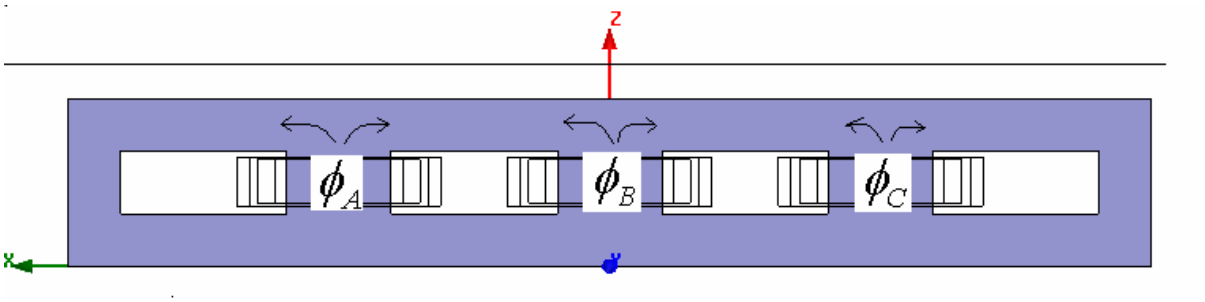

Figure 23 Fluxes "Spill Over" to the Outer Legs

4.4.2 Magnetizing Inductance Analysis

Magnetizing Inductance is also called mutual inductance, represents energy stored in the finite permeability of the magnetic core and in small gaps where the core halves come together. In the equivalent circuit, mutual inductance appears in parallel with the windings. The energy stored is a function of the volt-seconds per turn applied to the windings and is independent of load current. The equation to calculate the magnetizing inductance is as follow:

$$L_M = \frac{n_1^2}{\frac{l_c}{\mu \cdot A_c} + \frac{l_g}{\mu_o \cdot A_c}}$$

, where L_M=magnetizing inductance, n_1=primary turns, l_c=length path of core, l_g=length path of air gap, μ =permeability of the core, μ_o =permeability of air which is $4\pi \cdot 10^{-7} \frac{H}{m}$ and A_c=cross-sectional area of the core.

4.4.3 Leakage Inductance Analysis

The flux lines which link the primary but are diverted between coils so that are lost to the secondary represent induced voltage lost to the load. Some of the flux passes through the body of the primary coil and does not effectively link all of the primary turns; some of the flux passes through the body of the secondary coil and does link some of the turns.

Leakage inductance delays the transfer of current between switches and rectifiers during switching transitions. These delays, proportional to load current, are the main cause of regulation and cross regulation problems. However, the leakage inductance is needed for power transfer within the DAB. The leakage inductance formula is given as follow [9]:

$$R_C = \frac{F}{\phi} = \frac{l_C}{\mu \cdot A_C}$$

, where R_C =reluctance of core, F = magnetomotive force, ϕ =Flux, μ =permeability of the core, l_c=length path of core and A_c=cross-sectional area of the core

$$L_{11} = \frac{N_1^{\,2}}{R_{air1}} + \frac{N_1^{\,2}}{R_c} \text{ and } L_{22} = \frac{N_2^{\,2}}{R_{air2}} + \frac{N_{2^2}}{R_c}$$

, where L_{11} =self inductance of coil 1, L_l =reluctance of air path around coil 1, L_{22} =self inductance of coil 2, R_{air2} =reluctance of air path around coil 2

$$k = \frac{|L_{12}|}{\sqrt{L_{11}L_{22}}}$$

, where k=coefficient of coupling

$$L_{leak} = (1-k)L_{11}$$

, where L_{leak} =leakage inductance

Due to the leakage inductance changes with length path of the air of coil 1 and 2 which is the geometry of the winding, it is hard to measure and time consuming process. So the leakage inductance is calculated from the Finite Element Analysis (FEA) by Anosft® Maxwell® 3D software.

Table 24 Inductance simulated by Maxwell 3D®

Design	Topology 1		Topology 2	
	33.3 kVA@3 kHz	33.3 kVA@20 kHz	100 kVA@3 kHz	100 kVA@20 kHz
L_{11} [mH]	14.1910	2.810819	33.9700	8.27789
L_{22} [mH]	2.7913	0.283068	2.29	0.562224
L_{12} [mH]	482.02	19.91865	950.25	197.85
L_{leak} [mH]	3.4252	1.904	5.36	1.77
Required L_{leak}[mH]	30.084	4.513	9.0251	1.3538
$L_{inductor}$ [mH]	26.6588	2.609	3.6651	N/A

Because of the closely coupled between the primary and secondary windings, the leakage inductances are relatively small which require an external inductor connected in series with the primary winding to make up for the inductance needed for the power transfer in the DAB converter.

4.5 Inductor Design

To make up the inductance for the lack of leakage inductance from the transformer design, an air inductor is designed for each of the topologies. Nomex® insulation is used for winding cylinder and layer insulation for the air inductor. The inductor's design is described below.

Table 25 Inductor Designs

	Topology 1 33.3 kVA	Topology 1 33.3 kVA	Topology 2 100 kVA
Inductance [mh]	26.6588	2.609	3.6651
Voltage	3800	3800	11400
Current	2.92	2.92	2.92
Frequency [f]	3000	20000	3000
Conduct [AWG]	#14	#26	#14
Conduct in parallel	1	10	1
Turns	857	380	206
Turns per Layer	86	10	42
Number of Layers	10	38	5
ID	6.1	5.8	5.08
OD	13.05	7.66	9.93

Table 25 Continued

Winding Length [cm]	15.04	18.34	7.22
Conductor Length [m]	274	85.7	51.7
Conductor Weight [kg]	5.2	0.77	0.96
Conductor Loss [w]	24.5	15.8	4.6
Temperature Rise above 30 C Ambient	18.91	17.33	4.55

CHAPTER 5

5 INSULATION ANALYSES

Insulation is perhaps the most important part of a transformer, if indeed any part can be said to be most important, because insulation keeps the transformer from destroying not only itself but other equipments as well. If the performance of the transformer is poor in other respects, it will still perform its major function of transforming power, but insulation failure at any point is disastrous.

Perhaps the size of the core and coils is the most challenging process in this whole transformer design. In the current power system, the high frequency applications are still in the research and development stage and they are usually in the lower power and voltage range. Therefore, the selection for high power and high voltage materials are difficult to find. As discussed earlier, the size of the transformer core decreases as the operating frequency increases, at the same time the available core window size becomes less and less for the windings to fit and making the electrical insulation the most challenging process of this design.

There are several criteria the electrical insulation has to meet:

1 Adequate effective dielectric strength against various types of voltages – operating, system fault, etc.

2 Adequate coil ventilation.

3 Adequate mechanical strength.

4 Minimum cost.

5.1 Electric Breakdown and Partial Discharge

The insulation must be designed to withstand all voltages stress in the transformer. Usually air is a very good insulating material. However, when a critical electric field is exceeded, conduction paths grow at microsecond speeds through the air, in the form of branched trees, called streamers. These can lead to destructive breakdown.

Spark is triggered when the electric field strength exceeds approximately 4-30 kV/cm for air. This may cause a very rapid increase in the number of free electrons and ions in the air, temporarily causing the air to abruptly become an electrical conductor. This is also called dielectric breakdown. Therefore, different types of insulation materials with higher electric field strength than air are implemented in this design to leave enough margins to prevent failure mode.

Since the transformer is dry-type design, insulating by air, partial breakdown of the air occurs as a corona discharge on high voltage conductors at points with the highest electrical stress. As the dielectric strength of the material surrounding the conductor determines the maximum strength of the electric field the surrounding material can tolerate before becoming conductive. Generally speaking, insulating materials have much more strength than can be used because it is practically impossible to design insulation structures that will stress the insulation uniformly.

5.2 Insulation Strategy

There are two topologies proposed in this thesis, hence there are two input voltages for each design; 3.8 kV and 11.4 kV for Topology 1 and 2 respectively and output voltage of 750 V. However, due to the dual active bridge voltage level requirement, the

transformer is designed for the worst case 11.4 kV phase-to-ground on the high voltage side and 750 V phase-to-ground on the low voltage side for both topologies with the exception of line-to-line voltage level for topology 2, is insulated at $\sqrt{3}$ *11.4 kV=20 kV between HV windings is designed.

Basically, there are four different types of insulation material that are used in this transformer design. The conductor itself has a thin coating of Polyurethane, which is able to withstand 200 V between conductor and conductor. The second insulation is sheet of DuPont™ Nomex® type 410 insulation, is used for the most part of the transformer process. Its high inherent dielectric strength, mechanical toughness, flexibility and resilience properties are particular friendly to the transformer. Its high dielectric strength is sufficient for this transformer application except where core window space is limited for the 11.4 kV high voltage design. The electrical property table is described below, Figure 11. DuPont recommends that continuous stresses in transformers not exceeding 1.6 kV/mm (40 V/mil) to minimize the risk of partial discharges (corona) [12]. This is the rule of thumb when sizing the insulation for this material.

TYPICAL ELECTRICAL PROPERTIES

Nominal thickness (mil)	2	3	5	7	10	12	15	20	24	25.5	29	30
(mm)	0.05	0.08	0.13	0.18	0.25	0.30	0.38	0.51	0.61	0.65	0.73	0.76
Dielectric strength - AC rapid rise[1]												
(V/mil)	430	550	680	840	815	820	830	810	800	730	750	680
(kV/mm)	17	22	27	33	32	32	33	32	31	29	30	27
- Full wave impulse[2]												
(V/mil)	1000	1000	1400	1400	1600	N/A	1400	1400	N/A	N/A	N/A	1250
(kV/mm)	39	39	55	55	63	N/A	55	55	N/A	N/A	N/A	49
Dielectric constant[3] at 60 Hz	1.6	1.6	2.4	2.7	2.7	2.9	3.2	3.4	3.7	N/A	3.7	3.7
Dissipation factor[3] 60 Hz ($x10^{-3}$)	4	5	6	6	6	7	7	7	7	N/A	7	7

[1] ASTM D-149 using 50 mm (2 inches) electrodes, rapid rise; corresponds with IEC 243-1 subclause 9.1, except for electrode set-up of 50mm (2 inches)

[2] ASTM D-3426

[3] ASTM D-150

Figure 24 Electrical Properties of Nomex Insulation

For the high voltage 11.4 kV winding designs, the core window space does not allow enough room for the required thickness of Nomex® insulation. This is where the second insulation material comes in, Kapton®, which is also a DuPont™ product. The electrical property table is shown below [13]. It is shown that Kapton® has a superior dielectric strength for a given thickness compare to the Nomex® material. DuPont™ also states that this insulation is able to withstand a voltage of 425 V per mil without suffering a sign of corona. The corona voltage versus time is shown in the Figure 13. This is 10 times better than the Nomex® insulation. The transformer designer is able to have a more compact design without sacrificing the integrity of the transformer. In addition, the operating frequency has little effect on the dielectric constant of the insulating material for the operating temperature of this design which can be ignored.

Typical Electrical Properties of Kapton® Type HN and VN Films

Property Film Gauge	Typical Value		Test Condition	Test Method
Dielectric Strength	V/µm (kV/mm)	(V/mil)	60 Hz	ASTM D-149-91$^{\varepsilon 1}$
25 µm (1 mil)	303	(7700)	1/4 in electrodes	
50 µm (2 mil)	240	(6100)	500 V/sec rise	
75 µm (3 mil)	205	(5200)		
125 µm (5 mil)	154	(3900)		
Dielectric Constant			1 kHz	ASTM D-150-92
25 µm (1 mil)	3.4			
50 µm (2 mil)	3.4			
75 µm (3 mil)	3.5			
125 µm (5 mil)	3.5			
Dissipation Factor			1 kHz	ASTM D-150-92
25 µm (1 mil)	0.0018			
50 µm (2 mil)	0.0020			
75 µm (3 mil)	0.0020			
125 µm (5 mil)	0.0026			
Volume Resistivity	Ω·cm			ASTM D-257-91
25 µm (1 mil)	1.5×10^{17}			
50 µm (2 mil)	1.5×10^{17}			
75 µm (3 mil)	1.4×10^{17}			
125 µm (5 mil)	1.0×10^{17}			

Figure 25 Electrical Properties of Kapton

Voltage Endurance of 100HN Kapton® Polyimide Film*

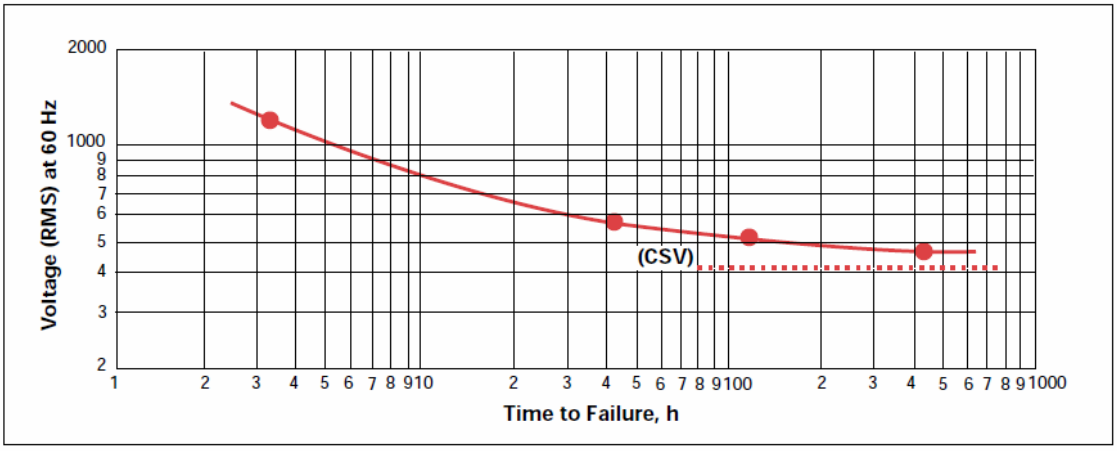

*Corona Starting Voltage (CSV) = 425 V

Figure 26 Corona Starting Voltage is 425 V for Kapton Insulation

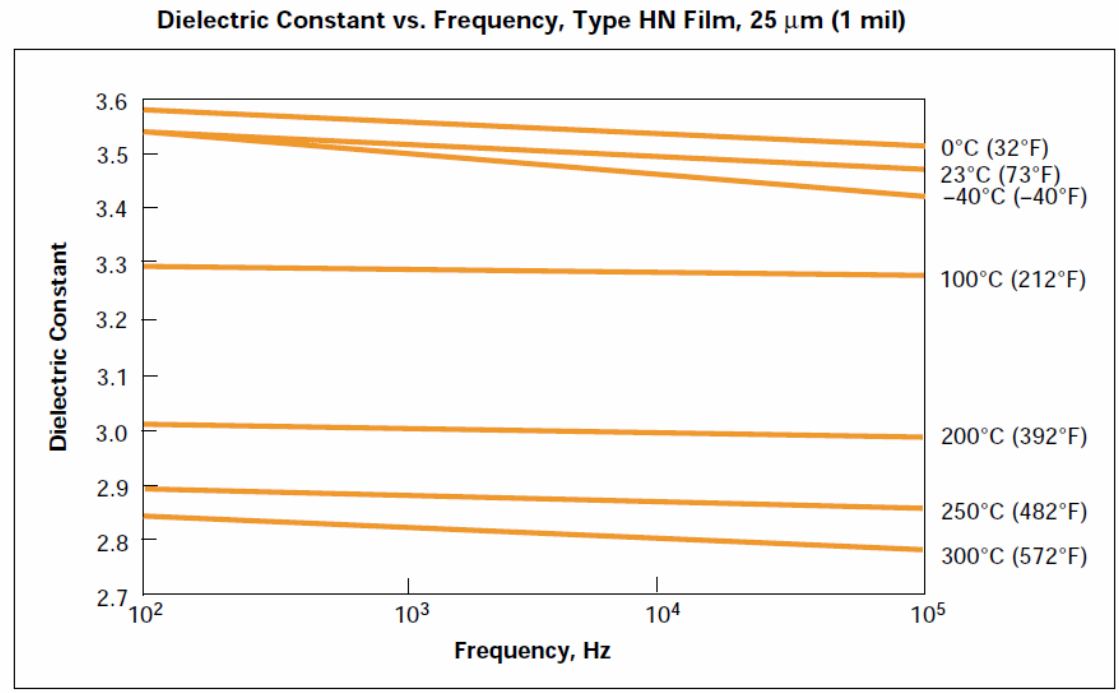

Figure 27 Dielectric Constant vs. Frequency for Kapton Insulation

The last insulation, air, is the most common insulating property in the electrical system. Air is used as the boundary of the core and coils throughout designs.

The insulation strategy is divided into several categories;

- For the Core-to-LV winding insulation, layers of insulation sheets wrap around the core for the winding cylinder, sharp points are of concern on the four core corners.
- The voltage difference between Turn-to-Turn varies as the flux density, etc, changes in each design. Please see the table below for each design value.

- The voltage difference between Layer-to-Layer varies as the Turn-to-Turn changes and number of turns per layer changes in each design. Please see the table below for each design value.
- LV winding-to-HV winding, HV phase-phase and HV winding-to-Outer core legs are insulated by sheets of insulation sandwiched between each other.

Table 26 Actual and Design Voltage Stress of Topology 1 – 3 kHz 33.3 kVA

	Actual Voltage Stress [V]	Design Withstand Voltage [V]	Design Thickness [mm]	Type of Material
Core-to-LV Winding	750	11520	7.2	Nomex®
LV Turn-to-Turn	23.4	200	0.127	Polyurethane
LV Layer-to-Layer	94	120	0.0762	Nomex®
LV winding-to-HV winding	11400	11520	7.2	Nomex®
HV Turn-to-Turn	23.4	200	0.127	Polyurethane
HV Layer-to-Layer	280	280	0.1778	Nomex®
HV phase-to-phase and HV winding-to-Outer core	19750	20400	1.2	Kapton®

Table 27 Actual and Design Voltage Stress of Topology 1 – 20 kHz 33.3 kVA

	Actual Voltage Stress [V]	Design Withstand Voltage [V]	Design Thickness [mm]	Type of Material
Core-to-LV Winding	750	11520	7.2	Nomex®
LV Turn-to-Turn	15.16	200	0.127	Polyurethane
LV Layer-to-Layer	30.32	80	0.0508	Nomex®
LV winding-to-HV winding	11400	20400	1.2	Kapton®
HV Turn-to-Turn	15.16	200	N/A	Polyurethane
HV Layer-to-Layer	75.8	80	0.127	Nomex ®
HV phase-to-phase and HV winding-to-Outer core	19750	20400	1.2	Kapton®

Table 28 Actual and Design Voltage Stress of Topology 2 – 3 kHz 100 kVA

	Actual Voltage Stress [V]	Design Withstand Voltage [V]	Design Thickness [mm]	Type of Material
Core-to-LV Winding	750	4800	3	Nomex ®
LV Turn-to-Turn	39.03	200	0.127	Polyurethane
LV Layer-to-Layer	78.06	80	0.0508	Nomex®

Table 28 Continued

LV winding-to-HV winding	11400	22800	2	Kapton®
HV Turn-to-Turn	39.03	200	0.127	Polyurethane
HV Layer-to-Layer	625	850	0.0508	Kapton®
HV phase-to-phase and HV winding-to-Outer core	19750	20400	1.2	Kapton®

Table 29 Actual and Design Voltage Stress of Topology 2 – 20 kHz 100 kVA

	Actual Voltage Stress [V]	Design Withstand Voltage [V]	Design Thickness [mm]	Type of Material
Core-to-LV Winding	750	4800	3	Nomex®
LV Turn-to-Turn	32.16	200	0.127	Polyurethane
LV Layer-to-Layer	32.16	80	0.0508	Nomex®
LV winding-to-HV winding	11400	51000	3	Kapton®
HV Turn-to-Turn	32.16	200	0.127	Polyurethane
HV Layer-to-Layer	160.8	850	0.0508	Kapton ®
HV phase-to-phase and HV winding-to-Outer core	19750	51000	3	Kapton®

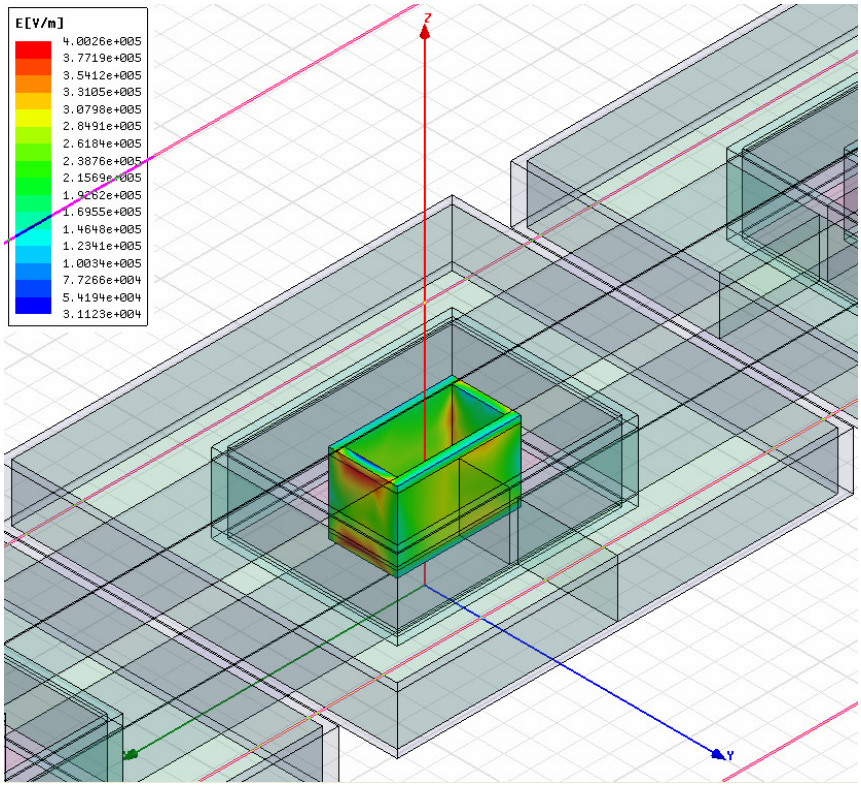

Figure 28 Insulation between Core and LV Winding (750V to Ground) in 3D view

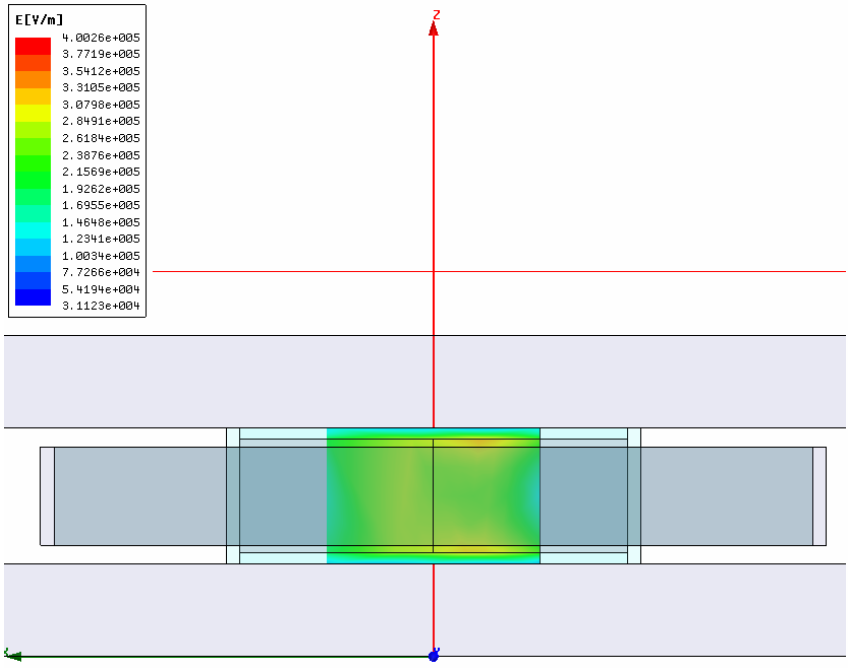

Figure 29 Insulation between Core and LV Winding (750V to Ground) in Top view

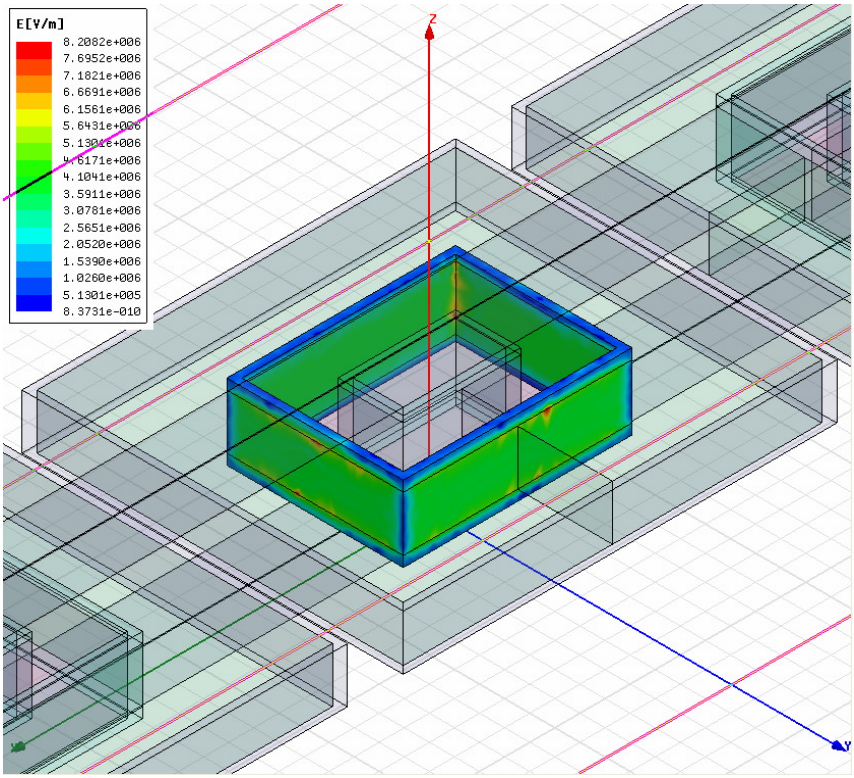

Figure 30 Insulation between HV and LV Winding (11400V to 750V) in 3D view

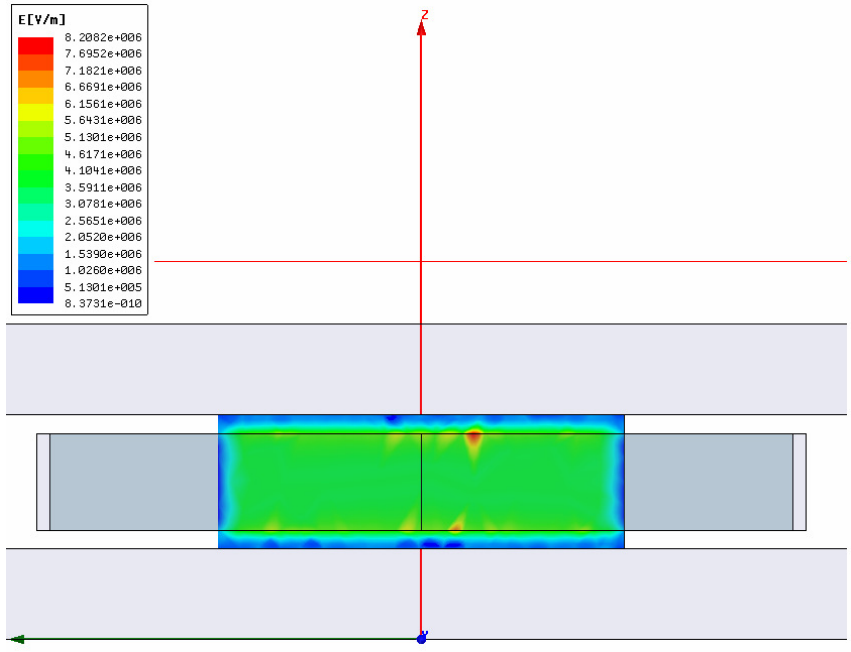

Figure 31 Insulation between HV and LV Winding (11400V to 750V) in Side view

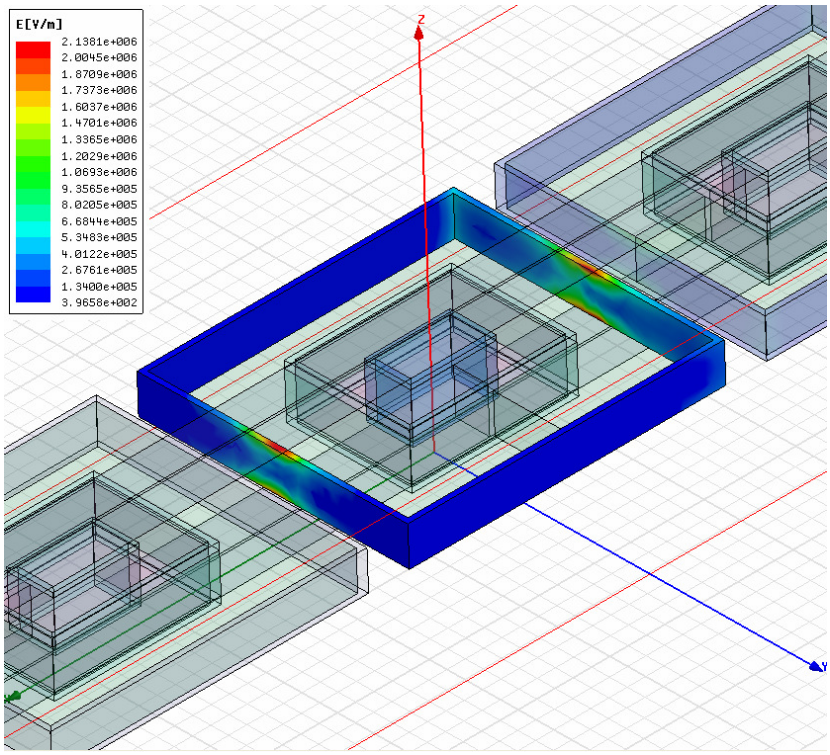

Figure 32 Insulation between HV and HV Winding (19745V to 19745V) in 3D view

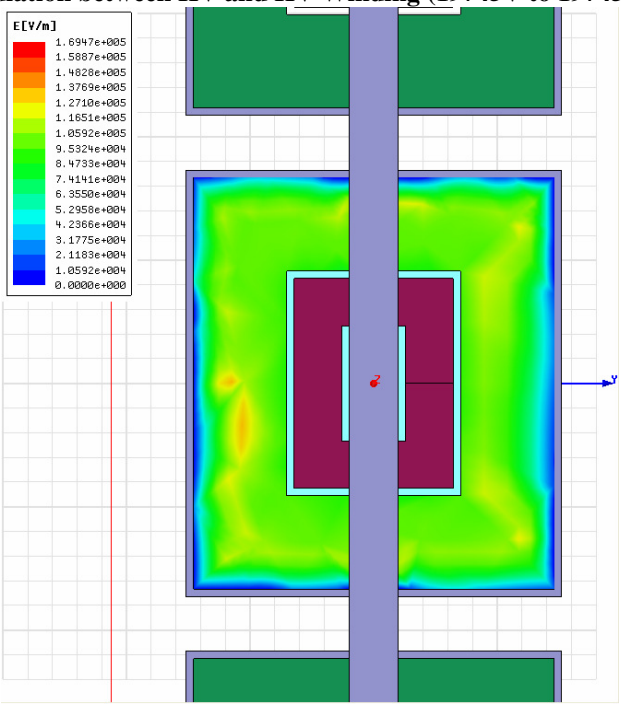

Figure 33 Insulation between HV Winding and Core (11400V to Ground) in Top view

CHAPTER 6

6 DIFFERENT TRANSFORMER DESIGN

6.1 3 Core Limbs with Tertiary Winding

In this paper, 3 phase high frequency transformer introduces the five limbs core to provide the additional magnetic return paths for the multiple of third harmonic flux in the fourth and fifth leg. The downside of this design is it requires more space than a three limbs core design. Another solution to capture the multiple of third harmonic flux is to provide a separate winding on each phase and connect the windings of all three phases in delta connection. These delta connected tertiary windings provide a low impedance path for the multiple of third harmonic to flow. This design also alters the waveform of the secondary side, since the Kirchhoff's voltage law around a closed loop states that the sum of the secondary line voltages (which are the secondary-coil voltages) must be zero. Therefore, there can be no third harmonic voltages in the secondary line voltages since third harmonic voltages cannot sum to zero. Keep in mind that the five core limbs design ensures the full primary voltage waveform get transfer to the secondary sides. Below is a cross-sectional diagram of the tertiary winding design.

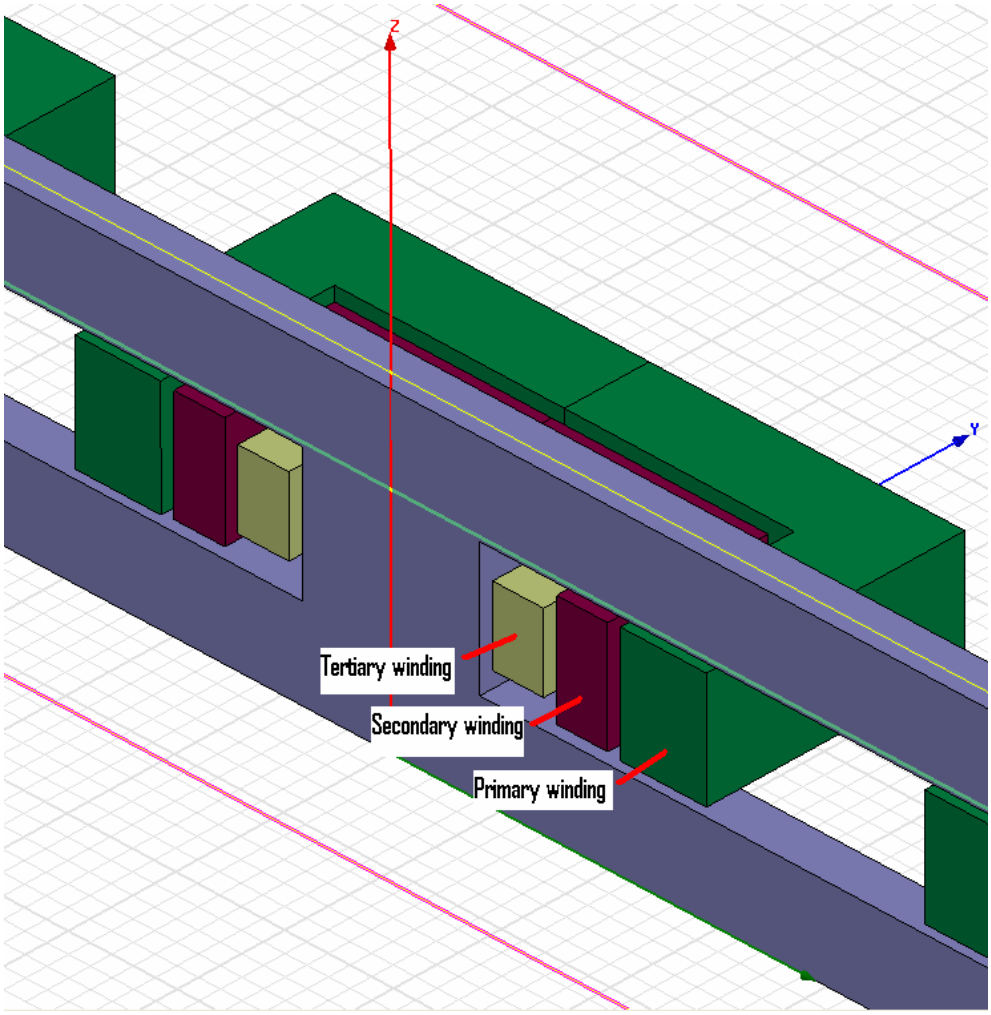

Figure 34 Tertiary Winding Design in cross-sectional view

6.2 Ferrite and Nanocrystalline Core Material Transformer Design

Matglas® is the main core material for this transformer design, because of its high flexibility in high saturation flux density and low material cost. However, this transformer design could not utilize the core's high saturation flux density, up to 1.56 Tesla, due to the temperature limitation in higher core loss result from higher flux density. So the ferrite core material becomes viable at lower flux density because of its lower core loss compare to the

Matglas® material. Also the nanocrystalline material is also another alternative due to its lowest core loss among the core material discussed if the material cost is not a factor in this design.

A comparison table is shown below to compare the core losses and size reduction between the Metglas®, ferrite and nanocrystalline core materials and different core designs. The 20 kHz and 33.3 kVA transformer design is chosen in this example.

Table 30 Size Comparison between Different Core Materials and Core Geometries

Core material	Metglas	Metglas	Ferrite	Nanocrystalline	
Configuration	5 limbs (Original)	3 limbs with tertiary	3 limbs with tertiary	3 limbs with tertiary	Units
Length	926	551	551	510	mm
Depth	156	140	140	134	mm
Height	70.8	70.8	70.8	70.8	mm
Winding losses	142	133	92	133	watt
Core Losses	160	169	136	86	watt
Leakage Inductance simulated by Maxwell® 3D	1.904	5.72	5.61	5.077	mH
Leakage Inductance required @ pi/6	4.513	4.513	4.513	4.513	mH
Leakage Inductance required @ pi/4	6.092	6.092	6.092	6.092	mH

The lengths of the core and coils do not change much because of the diameter of the windings governs the size of the core and coil. The core cross-sectional area is small for these designs anyways. For the better core materials like Nanocrystalline, as the core cross-sectional area decreases, the number of turns increases, more window area needed for windings. The number of turns in each design is preliminary fixed since the desire leakage

inductance is a function of a given number of turns. So the performance improvement comes in where the core losses is less for the better core material.

The core flux density screen shots are shown below between the 3 core legs, the 5 core legs, and 3 core legs with tertiary winding. The time of screen shot was chosen to see how the third harmonic flux affect the flux density in the core when all 3rd harmonic flux flow in the same direction, so the flux density is shown higher in both side of the top and bottom yoke.

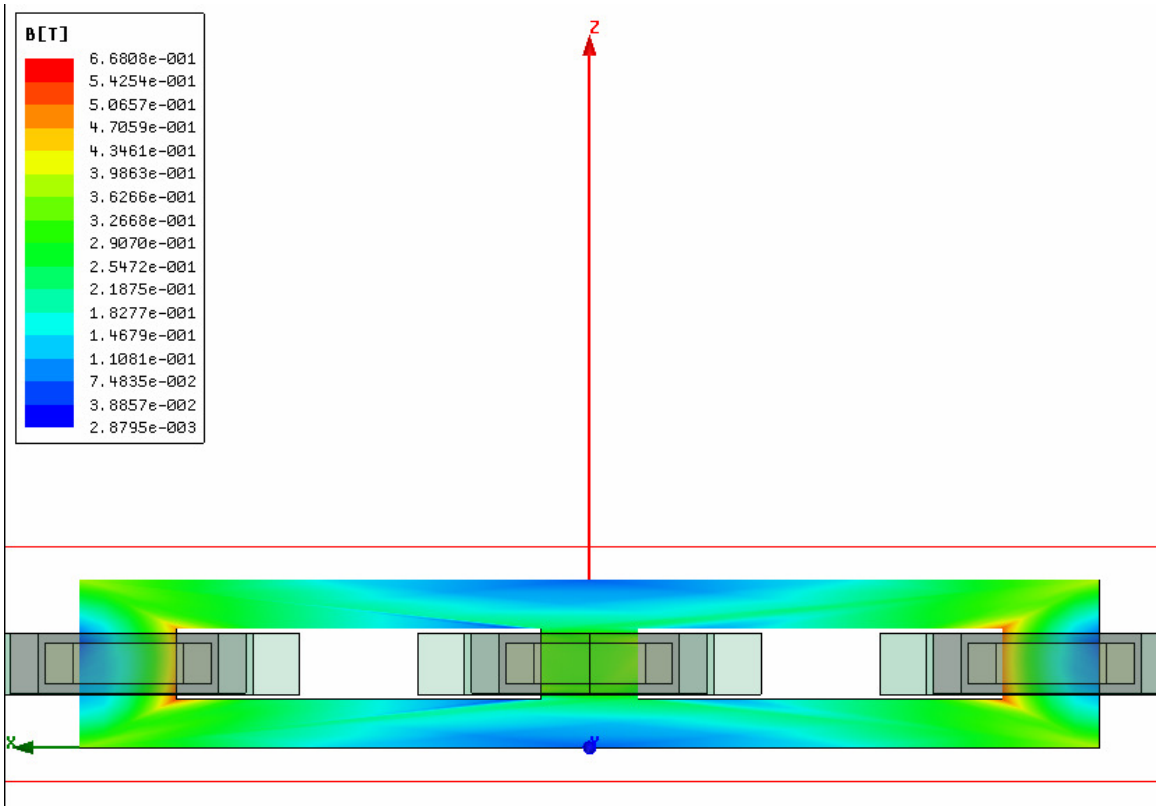

Figure 35 3 Core Limbs without Tertiary Winding

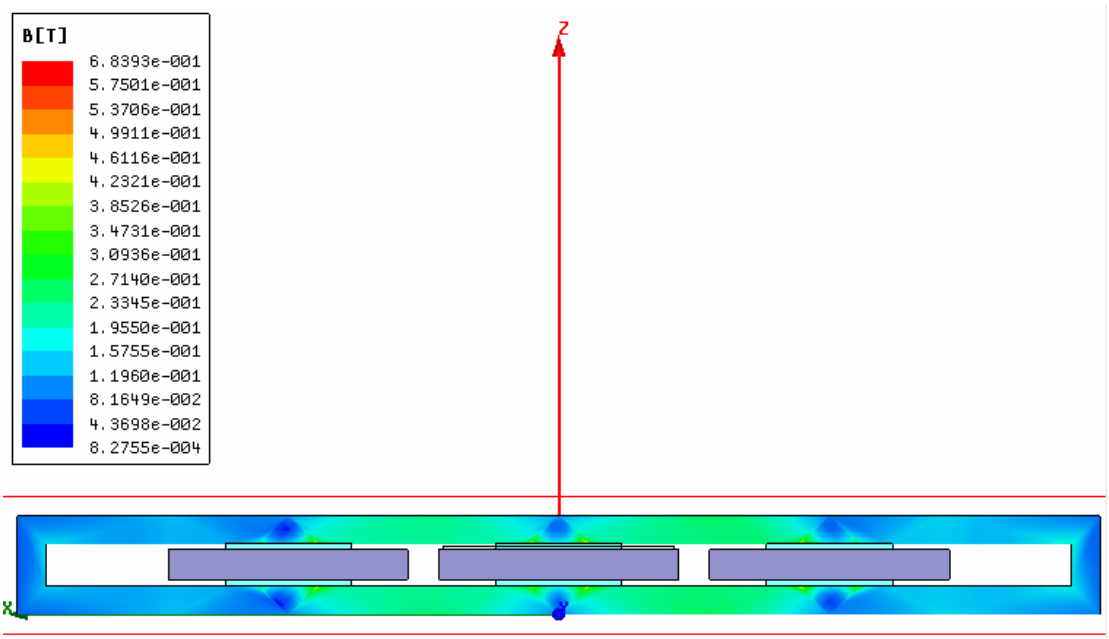

Figure 36 5 Core Limbs with Tertiary Winding

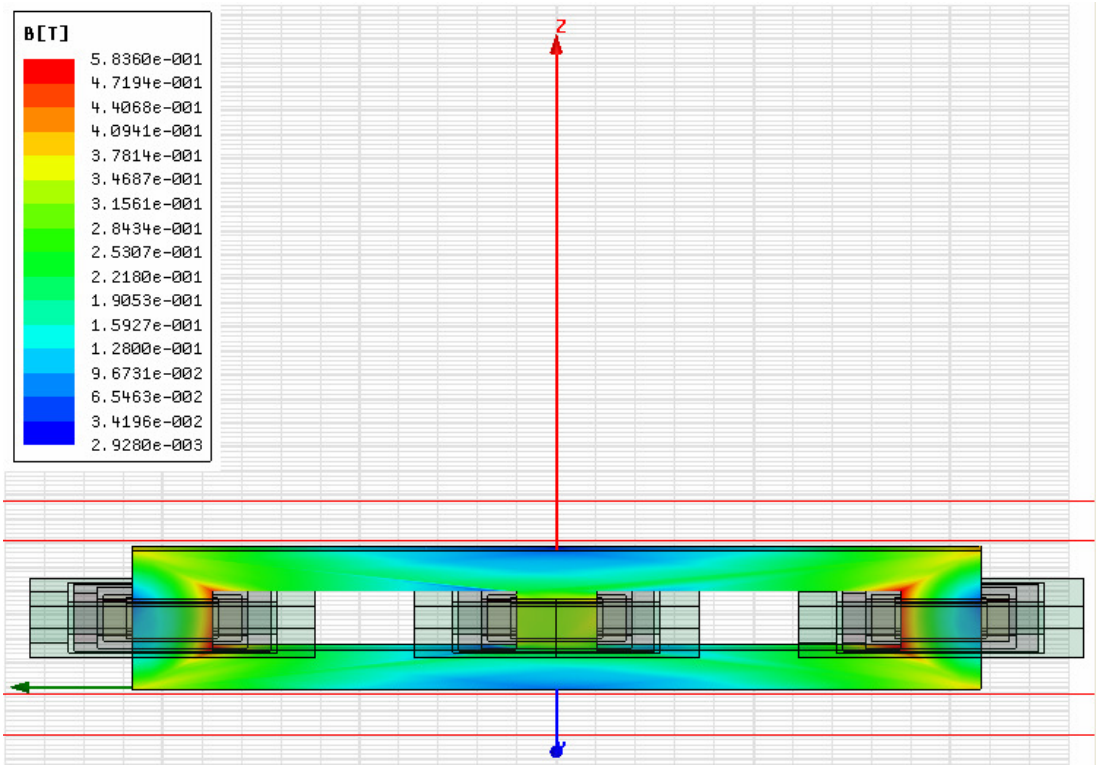

Figure 37 3 Core Limbs with Tertiary Winding

6.3 Three 3 phase 33.3 kVA in a Single Core

This design will further reduce the size of the transformer by combining all of the three stages of 33.3 kVA into one transformer. The inductance simulation is listed below.

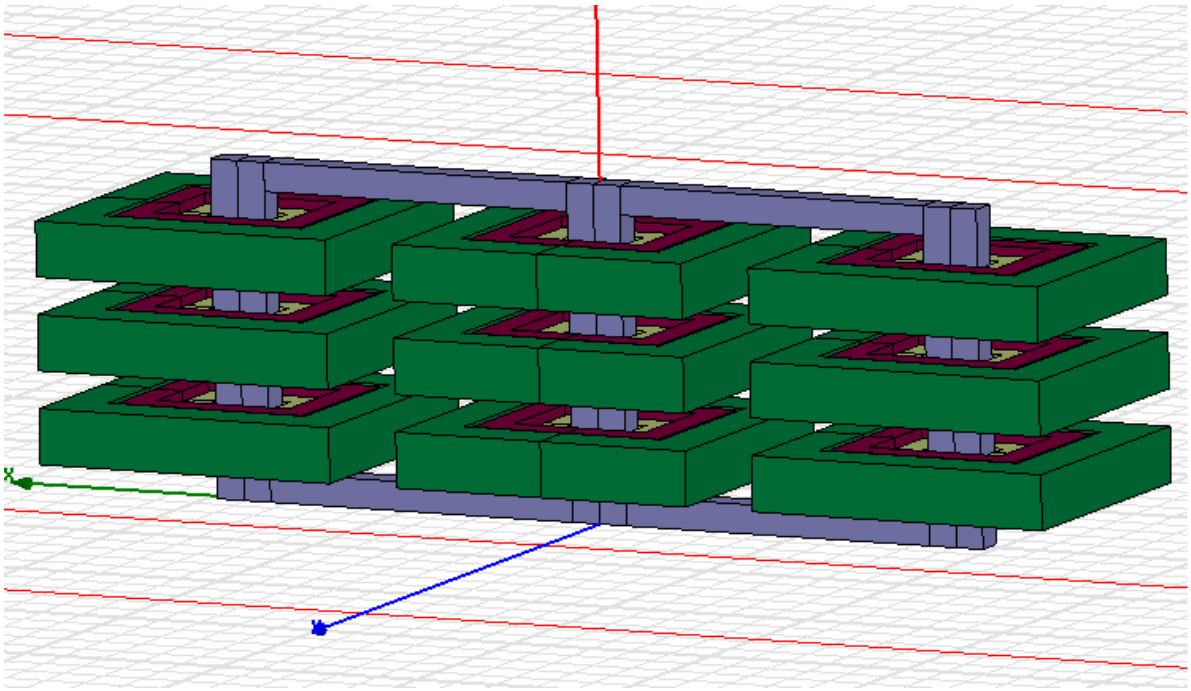

Figure 38 Three 3 phase 33.3 kVA in a Single Core

Table 31 Dimension of Three 3 phase 33.3 kVA in a Single Core Transformer

	Dimension
Width [mm]	556
Depth [mm]	124
Height [mm]	158

Table 32 Inductances simulation for Three 3 phase 33.3 kVA in a Single Core

Inductance [H]	HV Stage 1	HV Stage 2	HV Stage 3	LV Stage 1	LV Stage 2	LV Stage 3
HV Stage 1	0.069185	0.068267	0.067825	0.135.08	0.1344	0.13366
HV Stage 2	0.068267	0.69068	0.68267	0.13444	0.13486	0.13443
HV Stage 3	0.67825	0.68267	0.69187	0.13366	0.1344	0.13508
LV Stage 1	0.13508	0.13444	0.13366	0.02687	0.026567	0.026368
LV Stage 2	0.1344	0.13486	0.1344	0.026567	0.026802	0.026567
LV Stage 3	0.13366	0.13443	0.13508	0.026368	0.026567	0.026871

Table 33 Inductances Comparison between Different Stages in Three 3 phase 33.3 kVA in a Single Core

	HV Stage 1	LV Stage 1	HV Stage 2	LV Stage 2	HV Stage 3	LV Stage 3
Self Inductance [H]	0.69185	0.02687	0.69067	0.02680	0.69188	0.02687
Mutual Inductance of the same phase and same stage [H]	0.135082	0.1541574	0.13483	0.1547834	0.135084	0.1543541
Ratio between Mutual Inductance of stage 1 and 2	1.005					
Ratio between Mutual Inductance of stage 1 and 3	1.011					
Leakage Inductance between the same stage and same phase of HV and LV[H]	0.006412		0.006067		0.006424	

Table 33 Continued

Leakage Inductance required @ pi/6 [H]	0.04513
Leakage Inductance required @ pi/4 [H]	0.00677
Leakage Inductance between HV stage 1 and LV stage 2 of the same phase [H]	0.00903
Leakage Inductance between HV stage 1 and LV stage 3 of the same phase [H]	0.01364

Since, the mutual inductance between the different stages of the same phase has interference on each other, it is important to separate them as far as possible. The preferable mutual inductance ratio between difference stages should be at least 5. The next section describes the solution to the three 3 phase 33.3 kVA in a single core design.

6.3.1 Solution to the Three 3 Phase 33.3 kVA in a Single Core

Since each of the three stages has its own mutual inductance between its primary and secondary windings, it is important to avoid the different stages of mutual inductance interact with each stages of the same phase. One solution is to separate the windings between

different stages as far as possible. A preferable ratio of mutual inductance of the different stages against the same stages HV and LV windings is 5 times to 10 times. However, this design requires a large distance separation between different stages. It violates the primary objective of this thesis; reduce the size of the transformer.

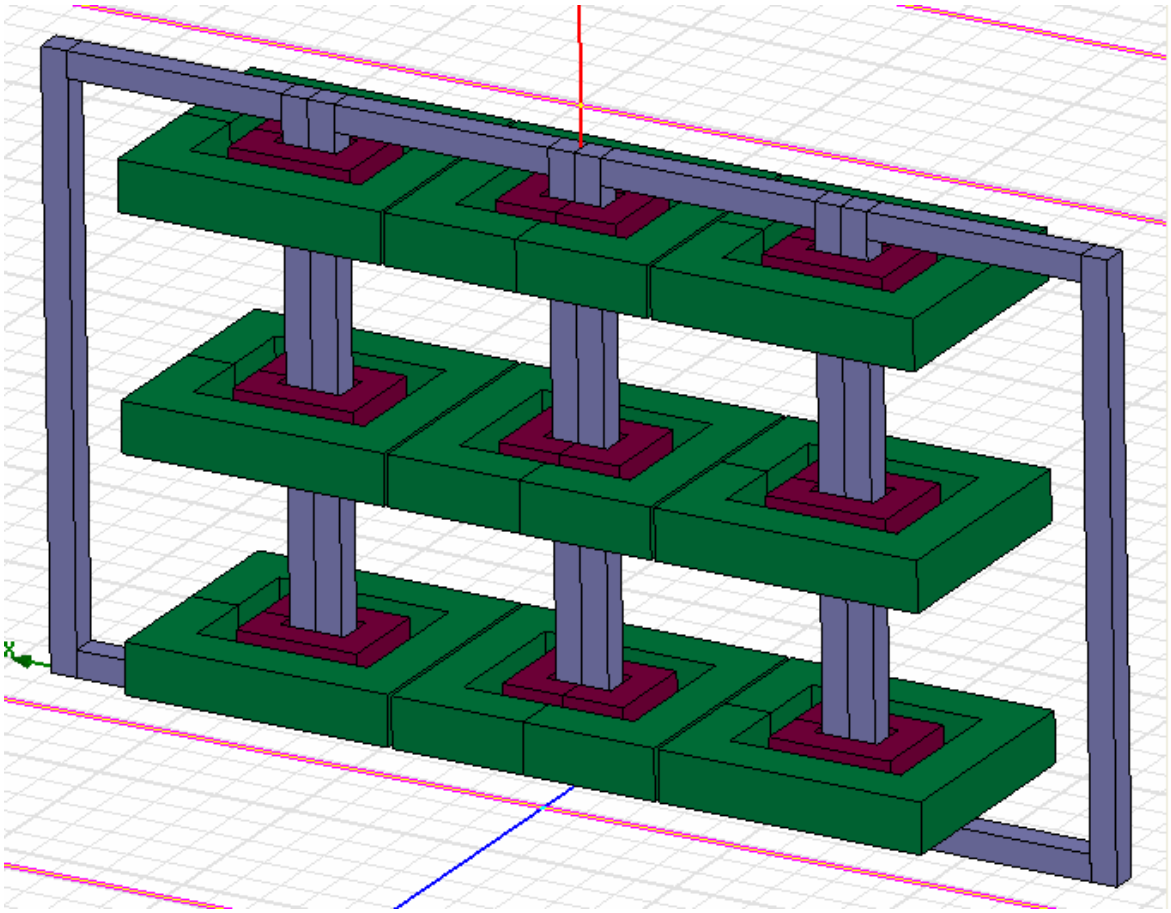

Figure 39 Alternate design of the Three 3 Phase 33.3 kVA in a Single Core

CHAPTER 7

7 CONCLUSION

7.1 Comparison

In this paper, two topologies and four designs have been proposed, analysis, simulated and verified. The objective of this paper was to find a design that deliver the most electricity, smallest physical size and the least inexpensive transformer design with the current technology available. As technology advances in power electronics, the power ratings of these devices have grown substantially to the point that kVA sizes of traditional 60 Hz transformer are able to conjunct with fast switching electronics. Power transformer is indispensible equipment in the power grids, voltages need to be step up and down throughout the long distance power grids in order to deliver electricity safely and economically. Utility companies are always looking for an alternative ways to generate and deliver electricity cheaply and environmental friendly.

Solid State Transformer (SST) is utilized the most advance technology available in conjunction with power electronics and high frequency transformer to step the voltage up or down and requires lesser storage space and material costs compare with a tradition 60 Hz transformer of the same rating. SST is a powerful device that is proven in technology and reliable for the user. SST has a high potential for more growth in the high power rating and high voltage applications in both the legacy power grids and renewable energy power grids.

Among the four designs in this paper, the two 3 kHz designs were able to design at higher flux density and less number of turns in the windings without sacrificing the core loss.

However, due to the closely coupled solenoid windings design, lesser number of turns led to lower leakage inductance value which an external inductor is required. On the other hand, the two 20 kHz designs needed to have a lower flux density to prevent high core loss and core loss has played an important role in the high frequency design as core surface area decreases with frequency increase and less core surface area to dissipate the heat to the surroundings. Lower flux density in the core was essential, however this ripple effect also led to higher number of turns in the winding. Inductances increase with number of turns in the windings. This tradeoff is benefitial to the DAB power transfer equation as leakage inductance approaches to the required value.

It is interesting fact to realize that the higher the operating frequency does not always give the most desire outcome. To compare between the 3 and 20 kHz of Topology 1 and 2 design, 20 kHz design uses a smaller core as one predicts, however, flux density needed to be low to prevent higher core losses as frequency is a exponential function of core loss. The tradeoff between conductor and core material is not justified in these 20 kHz designs. The 20 kHz designs' total weights are almost twice as much as the 3 kHz design and not much size reduction can be seen from the increase in frequency. In the ergonomics point of view, the 3 kHz designs are easier to manufacture as the core has a bigger window area to work with and the number of turns are smaller. The 3 kHz designs do not required as stringent insulation design as the 20 kHz since this is not as compact. Although, external inductors can be bulky in size, but the leakage inductance can be more controllable as the external inductor is an add-on device. Comparisons between the four designs are listed below.

Table 34 Design Parameters Comparison between all designs

	Topology 1	Topology 1	Topology 2	Topology 2
Power [kVA]	33.33	33.33	100.00	100.00
Frequency [f]	3000	20000	3000	20000
High Voltage [V]	3800	3800	11400	11400
Low Voltage [V]	750	750	750	750
HV Current [A]	2.92	2.92	2.92	2.92
LV Current [A]	14.789	14.789	44.367	44.367
Core Material Metglas® Powerlite®	AMCC 1000	AMCC 168S	AMCC 1000	AMCC 168S
Flux Density [T]	0.4	0.2	0.5	0.2
Number of Cores	4	4	4	12
Number of Primary Turns	173	355	414	355
Number of Secondary Turns	34	71	28	24
HV conductor size [AWG]	15	26	17	26
HV Conductor in Parallel	1	5	1	10
LV conductor size [AWG]	17	26	16	26
LV Conductor in Parallel	5	26	13	100
Core Weight [KG]	28.436	4.404	28.436	13.212
HV Conductor Weight[KG]	3.30	36.73	5.42	57.90
LV Conductor Weight [KG]	6.92	28.74	52.69	211.98

Table 34 Continued

External Inductor Weight [KG]	5.2	0.77	0.96	N/A
Overall Height [cm]	10.6	7.08	10.6	7.08
Overall Width [cm]	80.53	92.63	81.66	93.91
Overall Depth [cm]	22.53	15.60	23.66	60.87
Magnetizing Inductance [mH]	482.02	19.91865	950.25	197.85
Leakage Inductance [mH]	3.4252	1.904	5.36	1.77
Core Loss [W]	197	160	291	481
Winding Loss [W]	72	142	219	164
Total Loss [W]	269	302	510	645
External Inductor Loss [W]	24.5	15.8	4.6	N/A

REFERENCES

[1] Tiefu Zhao, Liyu Yang, Jun Wang, Alex Q. Huang. “270 kVA Solid State Transformer Based on 10 kV SiC Power Devices” IEEE Electric Ship Technologies Symposium, 2007. ESTS '07.

[2] Seunghun, Baek. “Design Considerations of High Voltage and High Frequency Transformer for Solid State Transformer Application”, North Carolina State University, 2009.

[3] H.K. Krishnamurthy, R. Ayyanar, “Building Block Converter Module for Universal (AC-DC, DC-AC, DC-DC) Fully Modular Power Conversion Architecture”, IEEE Power Electronics Specialists Conference, pp. 483-489, 17-21 June 2007.

[4] AK Steel®, “Oriented & TRAN-COR H, Electrical Steels”, AK Steel Corporation, 2007.

[5] Roya, R and A.K. Majumdara, "Thermomagnetic and transport properties of metglas 2605 SC and 2605", Journal of Magnetism and Magnetic Materials 25: 83-89, 1981.

[6] V.R. Ramanan, “Nanocrystalline soft magnetic alloys for application in electrical and electronic devices”, ABB-Electric Systems Techonology Institute. January 1998.

[7] John J. Winders, “Power transformer: Principles and Applications”, CRC Press, 2002.

[8] Robert M. Del Vecchio, Bertrand Poulin, Pierre T. Feghali, Diliphkumar M. Shah and Rajendra Ahuja, “Transformer Design Principles with Applications to Core-Form Power Transformers”, CRC Press, 2001.

[9] Alfred J. Goetze, “Introduction to Electric Power Systems”, North Carolina State University, 1991.

[10] “Powerlite® Technical Bulletin”, Metglas®, Inc., 2008.

[11] Richard L. Bean, Nicholas Chackan, Jr., Harold R. Moore, Edward C. Wentz, “TRANSFORMERS for the Electric Power Industry”, Westinghouse Electric Corporation, McGraw-Hill Book Company, Inc., 1959.

[12] “Nomex® Type 410 Technical Data Sheet”, DuPont®, 2003.